Microanalytical techniques for phenotyping secondary xylem

Nadeeshani Karannagoda [1] , Antanas Spokevicius [1] , Steven Hussey [2] , and Gerd Bossinger [1]

[1] School of Ecosystem and Forest Sciences, The University of Melbourne, Creswick, Victoria, Australia

[2] Department of Biochemistry, Genetics and Microbiology, Forestry and Agricultural Biotechnology Institute (FABI), University of Pretoria, Pretoria, South Africa

Abstract

The products of secondary xylem are of significant biological and commercial importance, and as a result, the biology of secondary growth and how intrinsic and extrinsic factors influence this process have been the subject of intense investigation. Studies into secondary xylem range in scale from the cellular to the forest stand level, with phenotypic analyses often involving the assessment of traits relating to cell morphology and cell wall chemical composition. While numerous techniques are currently available for phenotypic analyses of samples containing abundant amounts of secondary tissue, only a few of them (microanalytical techniques) are suitable when working with limiting amounts of secondary tissue or where a fine-scale resolution of morphological features or cell wall chemical composition is required. While polarised light microscopy, scanning electron microscopy, field emission-scanning electron microscopy and X-ray scattering and micro-tomography techniques serve as the most frequently used microanalytical techniques in morphotyping, techniques such as scanning ultraviolet microspectrophotometry, X-ray photoelectron spectroscopy, gas chromatography, Fourier-transform infrared spectroscopy and matrix-assisted laser desorption ionisation mass spectrometry serve as the most commonly used microanalytical techniques in chemotyping. Light microscopy, fluorescence microscopy, confocal laser scanning microscopy, transmission electron microscopy and Raman spectroscopy serve as dual micro morphotyping and chemotyping techniques. In this review, we summarise and discuss these techniques in the light of their applicability as microanalytical techniques to study secondary xylem.

Keywords: Wood; morphology; cell wall chemistry; extractives; small sample; microscopy; spectroscopy; phenotyping

INTRODUCTION

The secondary tissues wood and bark play significant roles in plant development. Secondary phloem is responsible for translocation of photosynthates and it shields and protects the plant from extreme temperatures, pests and pathogens. Secondary xylem is responsible for the transport of water and minerals from roots to crown, providing both rigidity and flexibility to allow trees to grow while adjusting to different environmental stimuli (such as gravity, wind

and light) and acting as one of the major carbon sinks on earth (Dejardin *et al.* 2010). As a renewable material, secondary xylem has numerous commercial applications including energy production (firewood and second generation biofuels), construction (timber and plywood for buildings and furniture) and pulp and paper production (Andersson-Gunneras *et al.* 2006; Dejardin *et al.* 2010; Ye and Zhong 2015). Because of its biological and economic significance, secondary growth has been extensively studied both in annuals such as *Arabidopsis* and in woody tree species (Chaffey *et al.* 2002; Groover and Robischon 2006; Zhong *et al.* 2010; Zhong and Ye 2013, 2014, 2015; Zhang *et al.* 2018).

Much research has been directed at understanding how cell/tissue structure, morphology and chemical composition changes in response to extrinsic (biotic and abiotic stresses) and intrinsic (genetic and epigenetic) factors. Also, in recent years, a substantial amount of research has focussed on lignocellulosic biomass due to the increasing interest in the use of lignocellulose in biofuel production. Examples include large scale population level experiments as well as fine scale experiments such as tissue or cellular level mapping and analysis of changes in cell morphology, cell wall chemical composition and/or micromechanical properties. Such efforts reveal how secondary xylem differentiation responds to seasonal, environmental and genetic variation, with respect to its physiology, molecular responses or plant growth regulator concentrations (Tuominen *et al.* 1997; Gierlinger *et al.* 2010; Taguchi *et al.* 2010; Gerber *et al.* 2016; Spokevicius *et al.* 2016; Wood *et al.* 2017; Felten *et al.* 2018; Kong *et al.* 2018). One common challenge faced by such studies is the selection of suitable methods to determine phenotypic changes specific to secondary xylem.

Selection of a suitable phenotyping method depends on the objective of the study, the nature of the sample (fresh or dried/preserved tissue), cost, number of samples and on the amount of tissue that is available for phenotyping. Of course, at the organismal level, individual trees can produce large amounts of tissue (gram or kilogram quantities), whereas, in the case of fine scale (micrometre) mapping across secondary xylem, the use of small tissue sectors derived from methods such as Induced Somatic Sector Analysis (ISSA) or when young plants are sampled, only microgram amounts of tissue are available for phenotyping (Gerber *et al.* 2016; Spokevicius *et al.* 2016). Compared to phenotyping unlimited amounts of tissue, only a few methods have proven suitable when analysing tissue samples in limited or small amounts or in cases where studying sample heterogeneity is important. In these instances, microanalytical characterisation becomes the only option.

Microanalytical techniques provide insights into morphological and chemical properties of secondary xylem where samples are limited to microgram quantities or less and can be broadly categorised into (i) methods for phenotyping morphological features (morphotyping) and (ii) methods for phenotyping chemical properties (chemotyping). Morphotyping can reveal anatomical features of wood cells such as cellular diameter, perimeter, cell size, cell length, cell shape, cell wall thicknesses, cell wall area and microfibril angle, and ultrastructural details such as different secondary cell wall layers and their distinct features. In contrast, chemotyping can provide details on chemical composition and the abundance and distribution of cell wall biopolymers (cellulose, lignin and hemicelluloses) and wood extractives (phenolics, tannins, terpenes, flavonoids and lignans). However, some specific techniques can be used both for morphotyping and chemotyping. Accordingly, this review describes some of the most widely used microanalytical techniques based on their ability to use small (μg or less) amounts of tissue for morphotyping, chemotyping or both (Fig. 1). We begin this review by highlighting some key aspects of sample preparation related to microanalytical techniques discussed below. We provide examples of how these microanalytical

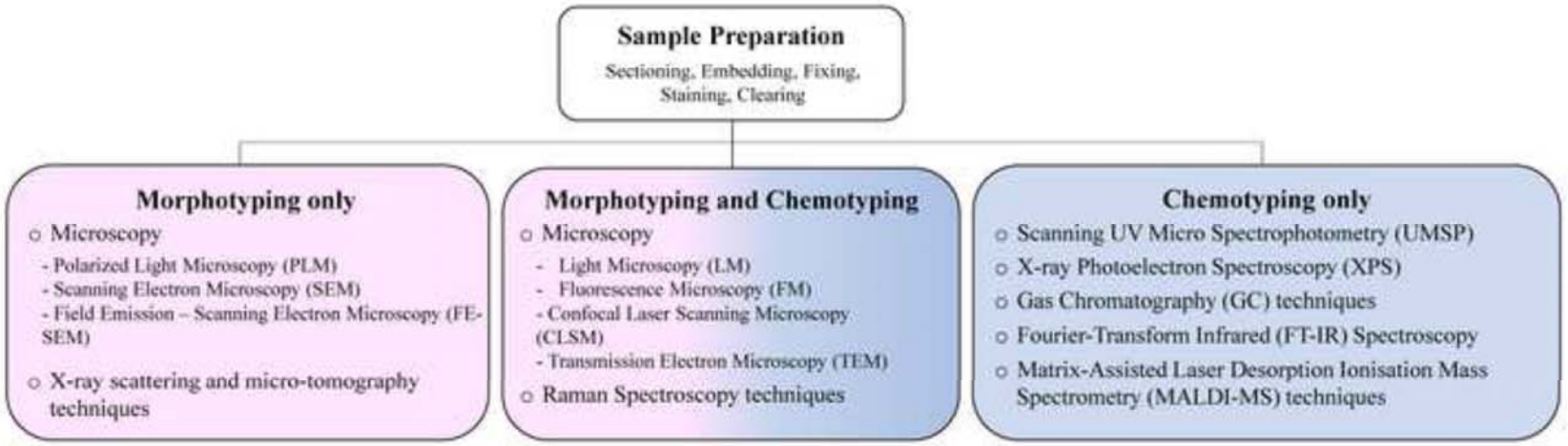

Figure 1. A summary of the key microanalytical techniques discussed in this review. Pink demonstrates microanalytical techniques for morphotyping, blue demonstrates microanalytical techniques for chemotyping, and pink/blue denotes dual micro morpho and chemotyping techniques. The pink and blue shading is consistent with that in Fig. 4.

techniques have been successfully used to phenotype woody tissue and present a comparative assessment of key microanalytical techniques together with a guide for the selection of techniques for specific applications.

Sample preparation

Sectioning, embedding and fixing

In this section, we outline some of the most used sample preparation methods and provide a summary relating them to the microanalytical techniques described in later sections (Table 4 and 5). Appropriate sample preparation is crucial to ensure that the quality and quantity of the sample suit the intended phenotyping method (Verhertbruggen *et al.* 2017). Depending on the intended phenotyping method, sample preparation could involve either a single step such as sectioning, grinding and milling or a sequence of steps such as fixing, embedding and sectioning. In preparation for certain applications like electron microscopy, the sectioned sample is subjected to additional steps such as dehydration, drying and sputter coating (with metals such as chromium, gold and/or platinum). Tissue maceration is another sample preparation method in which the cells/fibres are separated from one another by dissolving the middle lamella using chemicals such as glacial acetic acid, hydrogen peroxide, or nitric acid to name a few (Mahesh *et al.* 2015). Furthermore, for chemotyping purposes, samples can be ground to a powder (using a ball mill or similar) and/or chemically degraded/hydrolysed to separate soluble and insoluble fractions. For example, the chromatographic techniques such as gas chromatography (GC), require a sequence of labour-intensive sample preparation steps, generally starting from extraction followed by processing via hydrolysis, reduction and derivatisation (chemical reactions which can enhance the volatility of the sample components) (Angeles *et al.* 2006; MacMillan *et al.* 2015).

Tissue sections can be preserved by 'fixation' which terminates all cellular processes and immobilises cellular components to ensure that tissue sections remain close to their native state with all cells intact. Depending on the type of plant tissue and intended type of phenotyping, the requirement of a fixation step and appropriate type of fixation can vary. Fixation is only required in cases where intact cells/tissues are needed to analyse fine cellular features at the subcellular/organellar level. Fixation can be achieved either by chemical or physical means (i.e. dehydration), with the former using chemicals such as acetone, acetic acid, ethanol, methanol, glutaraldehyde, formaldehyde, glacial acetic acid or osmium tetroxide and the latter employing cryopreservation or microwaves (Bao *et al.* 2012; Begum *et al.* 2012; Yeung *et al.* 2015). With either method, consideration must be given to the potential introduction of fixation artefacts (cell shrinkage, cell swelling) which might influence the final outcome (Begum *et al.* 2012). One method of avoiding fixation artefacts is adjusting the osmolarity of fixation reagents to match that of the tissue (Loqman *et al.* 2010).

Tissue samples are often embedded to prevent distortion during subsequent sectioning steps. Use of a suitable embedding medium ensures that samples are sufficiently stabilised to withstand physical forces applied when sectioning using microtome-based methods or with laser microdissections. Commonly used embedding media include agarose, paraffin, LRwhite resin, polystyrene, polyethylene glycol, Spurr's resin and epoxy resin (Sato *et al.* 2001; Angeles *et al.* 2006; Wu *et al.* 2009; Bao *et al.* 2012; Begum *et al.* 2012; Yang *et al.* 2017). However, it must be noted that some embedding agents may not be suitable in all instances since they may interfere with a specific microanalytical technique where the embedding agent might become a contaminant (Foston *et al.* 2011). In such cases where embedding is not desirable, either a removable embedding medium (post sectioning) can be used or a

sectioning method that does not require embedding can be adopted, e.g. cryotome sectioning, which involves freezing tissue to increase its rigidity for sectioning (Foston *et al.* 2011).

Sectioning can be preceded by fixation, embedding, or a combination of both depending on the intended phenotyping method and required phenotypic data. Obtaining high quality sections with appropriate thicknesses is crucial for phenotyping since the quality of the section will have a considerable impact on the result. Sectioning can be performed by hand, by microtome (sliding microtome, rotary microtome, ultramicrotome, vibratome or cryotome) or by using laser microdissection, where methods like preparative laser capture micro-dissection have the potential to isolate microgram amounts of tissue potentially consisting of only a few cells (Angeles *et al.* 2006; Wu *et al.* 2009; Foston *et al.* 2011; Gerber *et al.* 2014; Lima *et al.* 2014; Yang *et al.* 2017). However, an alternative approach has been suggested by Dickson *et al*. 2017, which involves embedding the sample in resin and polishing it with a few different grinding papers. This approach precludes the need for sectioning and has proven to generate smooth surfaces which enable observation of subtle structures such as the cambium. The sectioned samples can then either be directly phenotyped or subjected to a preliminary staining step.

Staining

Staining allows rapid visual assessment of the integrity of tissues, cellular features and specific cell wall depositions. It has both morphotyping and chemotyping applications as stains can be used for visualisation of different chemical components in cell walls (e.g. polysaccharides, differences in lignin composition, differential staining of polysaccharides and lignin) and thereby allow for assessment of certain morphological features including cell wall thickness and cell size. (Wood 1980; Verbelen and Kerstens 2000; Lafarguette *et al.* 2004; Patten *et al.* 2005; Qiu *et al.* 2008; Anderson *et al.* 2010; Dogu and Grabner 2010; Mitra and Loque 2014; Kidner *et al.* 2016; Eckert *et al.* 2019; Smetana *et al.* 2019; Wessels *et al.* 2019; Yuan *et al.* 2019; Zhong *et al.* 2019). Commonly used stains include histological stains, fluorescent stains, immunological stains and metal-based stains where the choice of stain/staining depends on the features of interest and phenotyping method. Since some of these stains have toxic effects; special care must be taken when handling them.

Histological stains are the most used type of stains, and some of them are employed in light microscopy (LM) (Table 1). These histological stains can be used either for single or double staining (use of two stains to differentially stain two different types of cell wall polymers in contrasting colours) depending on cellular features of interest.

Fluorescent stains are another type of stain which are employed in fluorescence and confocal microscopy (Siebers 1960; Wood 1980; Stone *et al*. 1984; Brundrett *et al*. 1988, 1991; Kraus *et al*. 1998; Kitin *et al*. 2000; Moller *et al*. 2006; Bond *et al*. 2008; Anderson *et al*. 2010; Thomas *et al*. 2013; Pendle and Benitez-Alfonso 2015; Yeung *et al*. 2015; Sotiriou *et al*. 2016; Thomas *et al*. 2017; Morris *et al*. 2018; Schenk *et al*. 2018; Ursache *et al*. 2018; Wang *et al*. 2019). The fluorescence emitted from these stains can be easily distinguished from the scattering of the incident light, particularly if the incident light is monochromatic. Hence, if the sample itself possesses only a little or no fluorescence at a specific wavelength, then the entire intensity detected at that wavelength can be attributed to the fluorescent stain (Hubbe *et al.* 2019).

The challenging task of developing methods to selectively target specific cell wall polymers *in-muro*, has been significantly addressed by carbohydrate binding modules and immune-

Table 1 Commonly used histological stains for visualising cell wall polymers

Histological **stain**	**Chemical target**	**Colour after staining**	**References**
Safranin[†]	Lignin	Red	Begum *et al.* 2012, Carrillo *et al.* 2008, Gerber *et al.* 2014, Qiu *et al.* 2008, Sato *et al.* 2001, Smetana *et al.* 2019, Zhong *et al.* 2019
Phloroglucinol-HCl (Wiesner reagent)	Lignin	Characteristic pink	Araujo *et al.* 2014, Bao *et al.* 2012, Eckert *et al.* 2019, MacMillan *et al.* 2010, Wang *et al.* 2014, Yang *et al.* 2017
Mäule stain	Syringyl (S) lignin	Red	MacMillan *et al.* 2010, Patten *et al.* 2005
Toluidine blue O (TBO) (Stevenel's blue)	Pectin, Lignin, Tannins	Pinkish purple Greenish or bright blue	Bao *et al.* 2012, Chai *et al.* 2015, Kidner *et al.* 2016, MacMillan *et al.* 2010, Manabe *et al.* 2013, Mitra and Loque 2014, Patten *et al.* 2005, Yang *et al.* 2017, Wu *et al.* 2009
Congo red[†*]	β-(1→4)-glucans, Cellulose, Xyloglucan	Red	Mitra and Loque 2014, Verbelen and Kerstens 2000, Anderson *et al.* 2010, Wood 1980
Methylene blue	Cellulose	Blue	Al-Haddad *et al.* 2013, Chaffey *et al.* 2002, Kidner *et al.* 2016, Lafarguette *et al.* 2004, Qiu *et al.* 2008
Fast green	Cellulose	Green	Yuan *et al.* 2019, Zhong *et al.* 2019
Alcian blue	Insoluble carbohydrates, Non-lignified tissue	Blue	Smetana *et al.* 2019, Wessels *et al.* 2019, Al-Haddad *et al.* 2013, Chaffey *et al.* 2002, Kidner *et al.* 2016, Lafarguette *et al.* 2004, Qiu *et al.* 2008
Astra blue	Non-lignified polysaccharides	Blue	Carrillo *et al.* 2008, Groover 2016, Dogu and Grabner 2010

† Safranin and Congo red also has some fluorescent properties. * Congo red is considered as a weak stain for cellulose.

Table 2 Commonly used fluorescent stains for visualising cell wall polymers

Chemical target	Fluorescent stain	References
Callose	Aniline blue	Stone *et al*. 1984, Brundrett *et al*. 1988, Pendle and Benitez-Alfonso 2015, Sotiriou *et al*. 2016
Cellulose	Calcofluor white (fluorescent brightener)	Wood 1980, Anderson *et al*. 2010, Thomas *et al*. 2012
Cellulose	Pontamine fast scarlet 4B	Thomas *et al*. 2012, 2017
Cellulose, Xyloglucan	Congo red†	Wood 1980, Anderson *et al*. 2010, Thomas *et al*. 2012
Lignin	Safranin†	Kitin *et al*. 2000, Bond *et al*. 2008
Lignin, Callus	Basic fuchsin	Kraus *et al*. 1998, Moller *et al*. 2006, Ursache *et al*. 2018
Lignin, Suberin	Berberine	Brundrett *et al*. 1988, Yeung *et al*. 2015
Pectin	Coriphosphine	Siebers 1960, Morris *et al*. 2018, Schenk *et al*. 2018
Suberin	Fluorol yellow	Brundrett *et al*. 1991, Wang *et al*. 2019

† Safranin and Congo red also function as histological stains.

Table 3 Commonly used antibodies and carbohydrate binding modules in cell wall polymer detection

Specificity to epitopes in cell wall polymers	Antibody / Carbohydrate binding module	References
Callose ((1-3)-β-glucan)	(1-3)-β-oligoglucos -ides antibody, anti-1,3-β-glucan	Meikle *et al*. 1991, Altaner *et al*. 2010, Pendle and Benitez-Alfonso 2015
Cellulose (anti-amorphous)	CBM28	Blake *et al*. 2006, Ruel *et al*. 2012, Liu *et al*. 2013
Cellulose (crystalline)	CBM3a	Blake *et al*. 2006, Ruel *et al*. 2012, Liu *et al*. 2013, Qi *et al*. 2013, Yang *et al*. 2013
Cytoplasmic portion	JIM13	Yang *et al*. 2013
β-1,3-1,4-glucan	MLG	Liu *et al*. 2013
Galactan ((1-4)-β-galactan)	LM5	Willats *et al*. 2000, Arend 2008, Kim and Daniel 2017, Verhertbruggen *et al*. 2017
Mannan	LM21	Kim and Daniel 2017, Verhertbruggen *et al*. 2017
Heteromannan	BGM C6, LM22	
Xylan (4-O-methylglucuronoxylan), Heteroxylan (low substituted (1-4)-β-D-xylan)	LM10, LM11	Liu *et al*. 2013, Yang *et al*. 2013, Kim and Daniel 2017, Verhertbruggen *et al*. 2017
Xyloglucan	LM15	Kim and Daniel 2017
Arabinan in pectin ((1-5)-α arabinan)	LM6, LM13, LM16	Willats *et al*. 1998, Arend 2008, Snegireva *et al*. 2010, Kim and Daniel 2017, Verhertbruggen *et al*. 2017
De-esterified homogalacturonan	PAM1, CCRC-M38	Willats *et al*. 2000, Pattathil *et al*. 2010, Gritsch *et al*. 2015
Homogalacturonan in pectin		Clausen *et al*. 2003, Obro *et al*. 2007, Arend 2008, Snegireva *et al*. 2010, Liu *et al*. 2013, Yang *et al*. 2013, Verhertbruggen *et al*. 2017, Potocka *et al*. 2018
- high degree methylation	JIM7, LM20	
- low degree methylation	JIM5, LM19	
- partial methylation	LM18	

Arabinogalactan protein	JIM8, JIM13	Knox 1997, Zhang *et al.* 2003, Liebsch *et al*. 2014, Potocka *et al.* 2018
Arabinogalactan protein (tend to label cell walls or extracellular spaces)	Anti-AGPB	Zhang *et al.* 2003

staining. Immunostaining techniques use antibodies for detection of specific cell wall polymers and even specific decorations on polysaccharide backbones (Meikle *et al.* 1991; Knox 1997; Willats *et al.* 1998; Clausen *et al.* 2003; Zhang *et al.* 2003; Obro *et al.* 2007; Arend 2008; Altaner *et al.* 2010; Pattathil *et al.* 2010; Snegireva *et al.* 2010; Liu *et al.* 2013; Qi *et al.* 2013; Liebsch *et al.* 2014; Gritsch *et al.* 2015; Pendle and Benitez-Alfonso 2015; Kim and Daniel 2017; Potocka *et al.* 2018). Carbohydrate binding modules can detect polysaccharides and oligosaccharides such as cellulose and mannan. (Hilden *et al.* 2003; McCartney *et al.* 2004; Blake *et al.* 2006; Filonova *et al.* 2007). Some of the most commonly used antibodies and carbohydrate binding modules are listed in Table 3. The unique binding specificities of antibodies or carbohydrate binding modules towards cell wall polymers provide an excellent platform to determine the abundance and distribution of a polymer in cell walls. However, the signal reliability and interpretation can be influenced when certain antibodies fail to bind the targeted cell wall polymers either due to a structural alteration in the targeted cell wall polymer, due to masking of targeted cell wall polymer by other cell wall polymers or due to inaccessibility (Knox 2008; Sutherland *et al.* 2009).

Transmission Electron Microscopy (TEM) often employs metal stains such as lead citrate, uranyl acetate, osmium tetroxide and potassium permanganate. Lead citrate alters the contrast and thereby enhances structures in the final image to visualise cell wall polymer architecture. Uranyl acetate functions as a negative stain when looking at cellulose microfibrils whereas potassium permanganate functions as a positive stain for lignin (Sato *et al.* 2001; Lehringer *et al.* 2009; Bao *et al.* 2012). Osmium tetroxide, in particular, provides dark contrast areas which correspond to lignin or to its precursors on cell walls (Fig. 2h) (Hepler and Newcomb 1963; Borgin *et al*. 1975; Reza *et al*. 2014, 2015). Sometimes these stains are used in combination, e.g. the routine use of uranyl acetate and lead citrate in combination to achieve the highest contrast (Bao *et al.* 2012).

When observing secondary xylem under a microscope, ‘clearing' of tissue can enhance transparency of the specimen and reduce background signal, thereby circumventing light scattering which is the main hindrance to obtaining clear microscopic observations (Running *et al.* 1995; Gray *et al.* 1999; Kitin *et al.* 2000; Richardson and Lichtman 2015; Ariel 2017). Clearing agents are of two types; clearing agents like ethanol are used to remove the cellular cytoplasmic content whereas other clearing agents like lactic acid are used due to their ability to reduce refraction and light scattering during microscopy (Lux *et al.* 2005). However, it is crucial to choose a compatible solvent (glycerol, acetone, ethanol) for clearing since the use of unsuitable solvents can result in removal of the stain (Kitin *et al.* 2002, 2003). Similarly, the potential impact of certain solvents used in sample pre-treatment, such as excess stain removal, on wood properties, particularly the removal of soluble fractions via organic solvents, needs to be considered.

Morphotyping microanalytical techniques

Micro morphotyping techniques can reveal anatomical details such as cell size, cell shape, secondary cell wall thickness, microfibril angle, and ultrastructural details such as different secondary cell wall layers and their distinct features (Donaldson 2019). In this section, we describe some of the most widely used micro morphotyping techniques like polarised LM, electron microscopy and X-ray based techniques. For ease of reference, we summarise the features, inherent limitations, requirements and advantages of each technique in Table 4 and Fig. 4 to assist with the selection of a suitable micro morphotyping technique.

Table 4 Comparative assessment of microanalytical techniques that can be used to morphotype the secondary xylem

Properties	**LM/ PLM/FM**	**CLSM**	**SEM**	**FE-SEM**	**TEM**	**X-ray scattering/ µCT**	**Raman spectroscopy**
1. Sample thickness	µm	µm	µm	µm	nm	µm	µm
2. Sample preparation Hand sectioning (H), Microtomy (M)	H or M	H or M	H or M	M	M	M	M
3. Intact cellular structures after sample preparation	✓	✓	✓	✓	✓	✓	✓
4. Staining Chemical Stains (CS), Immuno Stains (IS), Fluorescent stains (FS)	LM - all, FM - FS, PLM - ×	CS, IS	-	-	CS, IS	-	-
5. Technical and labour demand	Low	Low	Low -Med	Med - High	Med - High	Med - High	Med - High
6. Potential throughput (relative to each technique)	High	High	Med - High	Med - High	Med - High	Med - High	Med - High
7. Chemotyping ability	✓	✓	×	×	✓	×	✓
8. Possible sample damage during imaging/analysis	×	✓	✓	✓	✓	✓[1]	×
9. Output Qualitative (QL), Quantitative (QN)	QL	QL	QL	QL	Both	QL	Both

1

10. Structural data Surface Structures (SS), Beneath Surface Structures (BSS)	SS	Both	SS	Both	Both	SS, BSS[I]	SS
11. Additional benefits i = Optical sectioning, ii = Single cell resolution, iii = 3D images, iv = Micromechanical properties	-	i, ii, iii	ii	i, ii, iii	ii, iii	iii[I], iv	ii, iv
12. Key references[#]	[1], [2], [3]	[4], [5], [6]	[7], [8], [9]	[10], [11], [12]	[13], [14], [15]	[16], [17], [18]	[19], [20], [21]

The above-discussed properties of LM are similar to those of PLM and FM except in the use of stains where PLM does not employ any stains and FM can employ fluorescent stains as well as fluorescently labelled immunostains. [I]Between X-ray scattering and µCT, only µCT is non-destructive, can analyse both surface and beneath the surface structures and generate 3D images. However, unlike X-ray scattering techniques, µCT cannot provide information on micromechanical properties. [#][1] Donaldson *et al*. 2010, [2] Oldenbourg 2013, [3] Verhertbruggen *et al*. 2017, [4] Bao *et al*. 2012, [5] Liu *et al*. 2017, [6] Kong *et al*. 2018, [7] Melder *et al*. 2015, [8] Yeung *et al*. 2015, [9] Kanbayashi and Miyanfuji 2016, [10] Lehringer *et al*. 2009, [11] Foston *et al*. 2011, [12] Derba-Maceluch *et al*. 2015, [13] Donaldson and Xu 2005, [14] Reza *et al*. 2015, [15] Xu *et al*. 2018, [16] Brodersen 2013, [17] Ruggeberg *et al*. 2013, [18] Saxe *et al*. 2014, [19] Gierlinger *et al*. 2010, [20] Perera *et al*. 2012, [21] Zhang *et al*. 2017

Table 5 Comparative assessment of microanalytical techniques that can be used to chemotype the secondary xylem

Properties	**UMSP**	**XPS**	**GC-MS**	**Py-GC (MS or FID)**	**FT-IR**	**MALDI-MS**
1. Sample thickness or weight	µm	µm-nm	µg	µg	µm-µg	µm-ng
2. Sample preparation Hand sectioning (H), Microtomy (M), Processing Steps (PS)[^], Laser Dissection (LD)	M	M	PS	H or LD	M	H or M
3. Intact cellular structures after sample preparation	✓	✓	×	✓	✓×[*]	✓
4. Technical and labour demand	Med - High	Med - High	High	Med - High	Med - High	Med - High
5. Potential throughput (relative to each technique)	Med - High	Med - High	Low	High	Med - High	High
6. Possible sample damage during imaging/analysis	✓	✓	✓	✓	×	✓
7. Output Qualitative (QL), Quantitative (QN)	Both	Both	QN	QN	Both	Both
8. Structural data Surface Structures (SS), Beneath Surface Structures (BSS)	SS	SS, BSS (<5 nm)	-	-	SS	SS
9. Additional benefits i = Optical sectioning, ii = Single cell resolution	-	i	-	-	ii	ii
10. Key references[#]	[1], [2], [3]	[4], [5], [6]	[7], [8], [9]	[10], [11], [12]	[13], [14], [15]	[16], [17], [18]

^ denotes processing steps such as extraction, hydrolysis, reduction and derivatisation. *✓× denotes instances in which sample can be used for analysis in several different forms such as sections or ground tissue. #[1] Koehler and Telewski 2006, [2] Carrillo *et al*. 2008, [3] Sandquist *et al*. 2015, [4] Inari *et al*. 2006, [5] Zuo *et al*. 2012, [6] Banuls-Ciscar *et al*. 2016, [7] Angeles *et al*. 2006, [8] Al-Haddad *et al*. 2013, [9] MacMillan *et al*. 2015, [10] Brodersen 2013, [11] Lourenco *et al*. 2013, [12] Lupoi *et al*. 2015, [13] Alonso-Simón *et al*. 2011, [14] Gorzsas *et al*. 2011, [15] Derba-Maceluch *et al*. 2015, [16] Obel *et al*. 2009, [17] Araujo *et al*. 2014, [18] Sturtevant *et al*. 2016

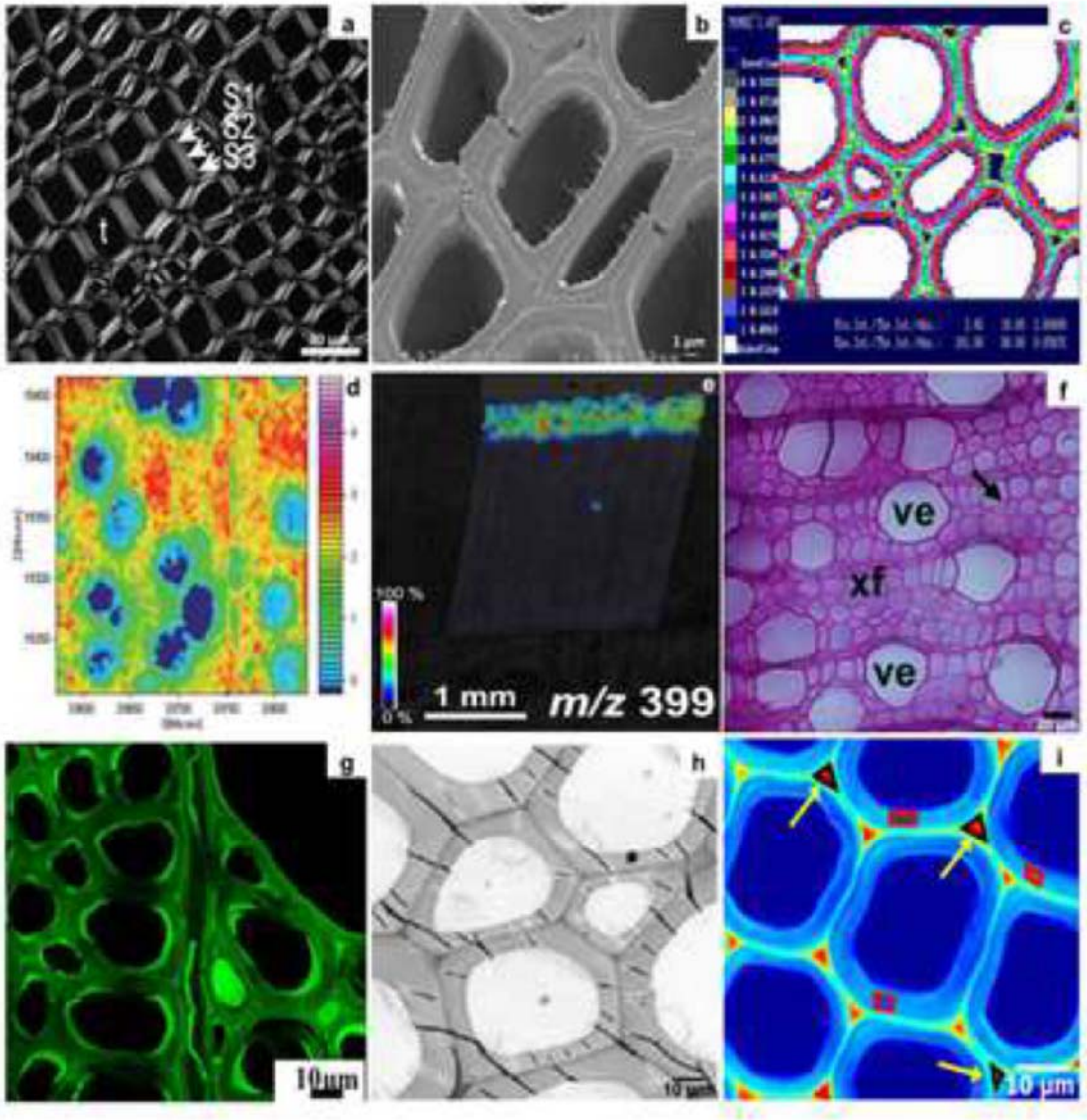

Figure 2. (a-i) Examples of wood samples subjected to different micro phenotyping methods. (a) PLM image of a transverse section of *Pinus radiata* juvenile wood demonstrating secondary cell wall layers (S1, S2 and S3), t denotes tracheid (adapted and reproduced with permission from Donaldson 2019). (b) FE-SEM micrograph of *Populus tremula* × *Populus tremuloides* stem cross section showing secondary cell walls of xylem fibres (kindly provided by Naoki Takata, Forestry and Forest Products Research Institute, Japan and Yuzou Sano, Hokkaido University, Japan). (c) UMSP scanning profile of *Acer* stem cross section showing lignin on xylem fibre and parenchyma cells, where the coloured pixels denote the absorbance intensity at 280 nm (kindly provided by Gabriele Ehmcke, Holzforschung München, Germany). (d) FT-IR spectral image showing lignin distribution in wood cells of *Fagus sylvatica* L., the colour scale demonstrates the lignin content from low (blue) to high (pink) (adapted and reproduced with permission from Müller & Polle 2009). (e) MALDI-MS ion image of a transverse section of differentiating *Chamaecyparis obtusa* xylem showing the distribution of coniferin (possible lignin precursor), where the colour scale indicates coniferin percentage (kindly provided by Arata Yoshinaga, Kyoto University, Japan). (f) LM image of *Populus tomentosa* stem cross section stained with phloroglucinol HCl, where the arrow indicates lignification and ve and xf denote vessels and xylary fibres, respectively (adapted and reproduced with permission from Yang *et al*. 2017). (g) CLSM image of poly(furfuryl alcohol)-treated *Populus euramevicana* stem cross section where fluorescence indicates the distribution of poly(furfuryl alcohol) on xylem cells (reprinted with permission from Kong *et al*. 2018, copyright (2018) American Chemical Society). (h) TEM micrograph of *Populus tremula* × *Populus tremuloides* stem cross section showing secondary cell wall thickness of xylem cells (adapted and reproduced with permission from Felten *et al*. 2018). (i) Raman spectroscopy image of *Pinus sylvestris* stem cross section; red squares in the cell walls denote the areas from where the cell wall spectra were extracted, while the triangles in the cell corners (pointed to by yellow arrows) denote the areas from where the cell corner spectra were extracted (adapted and reproduced with permission from Belt *et al*. 2017).

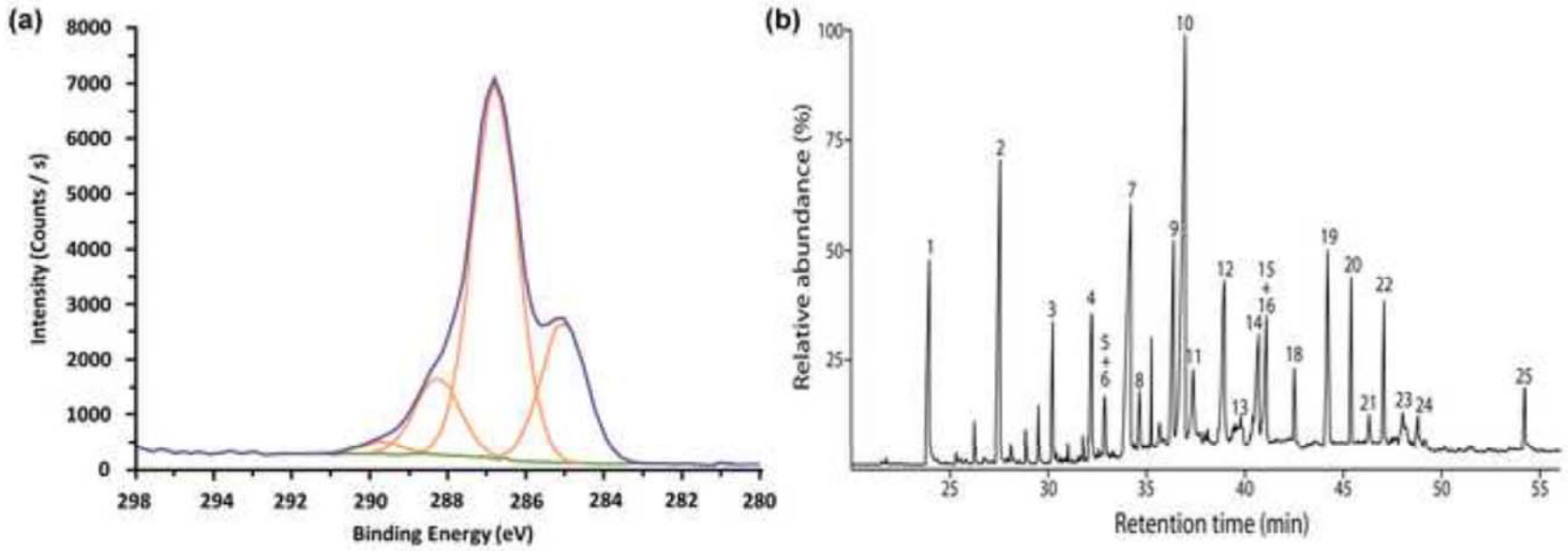

Figure 3. (a-b) Examples of non-imaging techniques used for micro phenotyping. (a) an XPS high-resolution spectra of *Pinus sylvestris* extracted hardwood (adapted and reproduced with permission from Bañuls-Ciscar *et al*. 2016). (b) Py-GC/MS chromatogram of *Quercus suber* L. xylem samples, the peaks labelled with numbers represent relative abundances of various lignin-derived compounds (adapted and reproduced with permission from Lourenço *et al*. 2016).

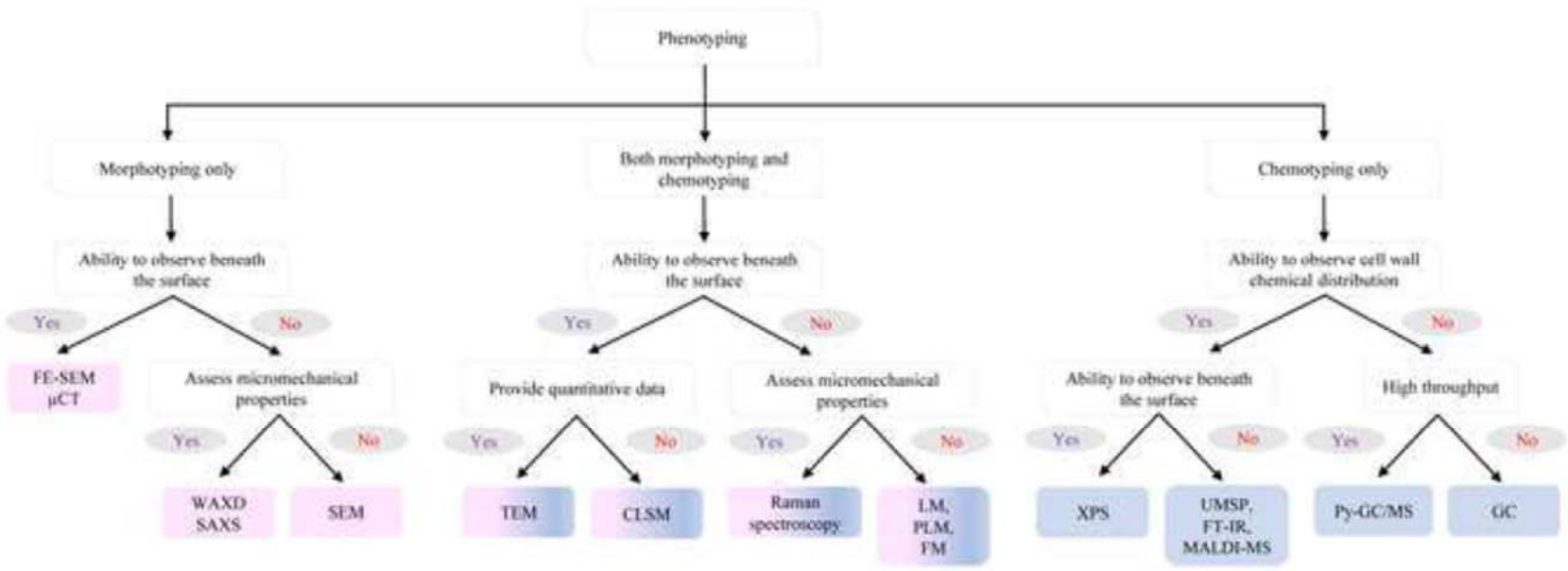

Figure 4. Selection guide for microanalytical techniques. Pink and blue shading is consistent with that in Fig. 1. The above properties of LM are similar to those of PLM and FM except in the use of stains where PLM does not employ any stains and FM can employ fluorescent stains as well as fluorescently labelled antibodies.

Polarised light microscopy (PLM)

Polarised light is a simple method that uses thinly sectioned or macerated (see section 1) samples and polarised light to observe cell wall layering and to inspect secondary cell walls which are birefringent owing to the orientated deposition of cellulose in contrast to the primary cell walls which are non-birefringent as a result of random cellulose deposition. Hence, polarised light circumvents the requirement for stains to distinguish cellular features (Preston 1974; Zhang *et al.* 2003; Oldenbourg 2013). Some applications of PLM include observation of different xylem cell types at varying developmental stages, microfibril angle, variations in secondary cell wall thickening and cellulose crystallinity (Fig. 2a) (Andersson *et al.* 2000; Zhang *et al.* 2003; Oldenbourg 2013; Olins *et al.* 2018; Donaldson 2019). PLM has been successfully used to measure microfibril angle, for example, in ISSA studies involving as little as 30 - 80 μg of wood sector material, demonstrating the high sensitivity of this method (Spokevicius *et al.* 2007; Lima *et al.* 2014). Similarly, polarised fluorescence microscopy also has been successfully used to measure microfibril angle (Verbelen and Kerstens 2000; Thomas *et al.* 2017). In addition, polarised fluorescence microscopy is also capable of estimating cell wall anisotropy (Altartouri *et al.* 2019).

Scanning electron microscopy (SEM)

SEM is the most commonly used microanalytical technique for observing surface features and anatomy of wood tissue sections and cells, typically at high spatial resolution and high magnification. Generally, in conventional SEM, achievable spatial resolution and magnification fall between 10 - 100 nm and 20× - 30,000×, respectively (Foston *et al.* 2011; Begum *et al.* 2012; Spokevicius *et al.* 2016). SEM fires a focused beam of electrons onto the surface of the sample and detects signals generated by electrons interacting with the sample to obtain information about the topography of the sample surface. Sample preparation can involve drying, fixing, sectioning and sputter coating or it can be as simple as just sectioning either by hand or by a microtome (Begum *et al.* 2012; Melder *et al.* 2015; Spokevicius *et al.* 2016). Sputter coating with gold, platinum or chromium makes samples more conductive and reduces charging, however, un-coated samples can be used if imaging can be done at low voltage mode, e.g. studies on xylem cell morphology that measures xylem cell features such as cross-sectional area, cell wall thickness and lumen area (Begum *et al.* 2012; Yeung *et al.* 2015; Kanbayashi and Miyafuji 2016; Spokevicius *et al.* 2016). SEM provides a pragmatic and relatively high throughput morphotyping platform to observe the ultrastructure of the secondary cell wall, the anatomy of wood cells and to accurately measure cellular dimensions.

Field emission-scanning electron microscopy (FE-SEM)

FE-SEM is a versatile, high-resolution microanalytical technique for morphotyping both surface and subsurface layers of secondary xylem. In particular, it can be used to morphotype tissue samples which are damaged due to mechanical handling (Singh and Dawson 2014). Compared to conventional SEM, FE-SEM employs a low acceleration voltage, a brighter electron source and a smaller beam size which typically improve the magnification and resolution up to 50,000× - 80,000× and 1 - 10 nm, respectively. However, the sample resolution also depends on sample preparation. As an example, sputter coating, which takes place after microtome sectioning, dehydration and drying of the samples, potentially adds ~10 - 20 nm to small structures. Heu *et al*. (2019) provide an excellent analysis of coating metals as a guide to select an optimum metal for sputter coating. As an example, the most suitable coating metals for high magnification and high-resolution FE-SEM imaging are chromium and tungsten. Although sputter coating may be disregarded, in the absence of sputter coating FE-SEM analysis may require a higher voltage and compared to a metal-

coated surface, the electron emission from a non-coated carbon surface is generally low. Hence an appropriate coating metal should be selected depending on the nature of the required analysis, which could be either microanalysis or imaging at high or low magnification (Heu *et al.* 2019).

In electron microscopy, charging artefacts often occur due to the tendency of electrons to accumulate within the sample resulting in an excess local signal. However, since FE-SEM can perform at low acceleration voltages, these charging artefacts can be reduced (Donaldson *et al.* 2007). When combined with a Focused Ion Beam (FIB), FE-SEM has the potential to provide micrographs with a resolution of as little as few angstroms, similar to that of a conventional transmission electron microscope. FE-SEM often serves as the method of choice for fibre cell analysis as it can be used to assess topography and anatomy of wood fibres (Fig. 2b), the arrangement of cellulose microfibres and microfibril angle (Lehringer *et al.* 2009; Foston *et al.* 2011; Derba-Maceluch *et al.* 2015; Takata *et al.* 2019). Although a higher magnification (> 80,000×) cannot be obtained without causing radiation damage and the delicate matter can be quickly degraded by the electron beam, FE-SEM has the potential to serve as a reliable and successful nanoscale platform for the analysis of tissue samples (Lehringer *et al.* 2009).

X-ray scattering and micro-tomography techniques

Wide Angle X-ray Diffraction (WAXD), Small Angle X-ray Scattering (SAXS) and X-ray micro-computed tomography (μCT) are some of the most commonly used X-ray based techniques. The WAXD and SAXS techniques are applied for elucidating structure and orientation of cellulose microfibrils, providing insights into the mechanical properties of tissue samples (Reiterer *et al.* 1999; Ruggeberg *et al.* 2013). X-ray scattering permits the use of samples in their native state rather than prepared samples, provides robust measurements and is high throughput, requiring about two minutes for measuring each angular step of 1.6º (Ruggeberg *et al.* 2013; Gerber *et al.* 2014). By adjusting the size of the beam, SAXS can be used at a spatial resolution on a micrometre scale or a bigger sample area comprising of several cells. However, the latter requires significant expertise in data interpretation as SAXS cannot differentiate between two cell types with different microfibril angles or the same cell type with two microfibril angles (Andersson *et al.* 2000; Reza *et al.* 2015). Radiation-induced damage is another drawback of X-ray based methods (Saxe *et al.* 2014). Nevertheless, SAXS and WAXS methods can provide insights into the cellulose arrangement of xylem cells. Some studies have used SAXS and/or WAXS methods to elucidate average microfibril angle in different secondary cell wall layers (e.g. S1 and S2), the average diameter of cellulose crystallites and the degree of crystallinity of cell wall layers (Andersson *et al.* 2000; Maloney and Mansfield 2010; Svedstrom *et al.* 2012; Gerber *et al.* 2014). However, such applications are not restricted to samples with secondary growth as SAXS can be successfully employed to elucidate microfibril angle in primary cell walls as well (Saxe *et al.* 2014). Furthermore, these techniques are often employed in X-ray based wood microdensitometry devices that analyse wood density and related anatomical features (Jacquin *et al.* 2017). For example, SilviScan is a device that combines an image analyser, an X-ray densitometer and an X-ray diffractometer which allows investigation of fibre morphology, wood density and microfibril angle, respectively (Evans 1994; Evans *et al.* 2000; Evans and Ilic 2001). In addition, μCT is a high-resolution and non-destructive technique for studying the 3D structure of wood which helps to visualise the spatial distribution and associations between different xylem cell types (Mayo *et al.* 2010; Brodersen 2013; Jacquin *et al.* 2017). Brodersen (2013) provides an excellent review of μCT in relation to wood anatomy.

Each micro morphotyping method has inherent constraints, requirements and potentials. Briefly, although PLM is convenient and straightforward, it fails to provide high resolution and magnification, which is crucial for morphotyping fine cellular structures. Though conventional SEM successfully addresses this drawback, it fails to reveal structural information beneath solid surfaces; however, this has been overcome by FE-SEM, as it enables imaging subsurface features. In addition to morphotyping, X-ray scattering has the potential to serve as a platform for investigating micromechanical properties of tissue specimens. Consequently, the selection of a suitable micro morphotyping method mainly depends on properties such as the required type of information, throughput/number of samples, physical effort, cost and skills required for data analysis and interpretation. Fig. 4 provides a decision guide that helps to select a suitable micro morphotyping method based on some of these properties.

Chemotyping microanalytical techniques

In addition to the need for qualitative or quantitative information, the selection of a micro chemotyping method depends on the scope of the study, the throughput of sample preparation, the complexity of data analysis and the ease of data interpretation. Further consideration must be given to the toxic nature of some chemicals, and how both chemicals and instruments can be handled safely. Micro chemotyping methods discussed under this section are employed to investigate the chemical characteristics of secondary xylem samples, such as particular polysaccharides and phenolics present in secondary cell walls (Willats *et al.*2000), without yielding morphotypic data.

Scanning ultraviolet microspectrophotometry (UMSP)

UV microscopy generates spectra for selected areas (usually resolutions of 0.25 × 0.25 μm) on tissue sections and the data derived from them can be employed in *in-situ* characterisation and/or semi-quantification of lignin and phenolics (Fukazawa 1992; Koch and Grunwald 2004; Irbe *et al.* 2006; Koehler and Telewski 2006; Carrillo *et al.* 2008; Foston *et al.* 2011; Sandquist *et al.* 2015; Ehmcke *et al.* 2017). Generally, sample preparation involves fixing, embedding and then sectioning (~ 1 μm thickness) (Irbe *et al.* 2006; Carrillo *et al.* 2008). For lignin detection, UMSP utilises the UV absorbance spectrum of lignin. As an example, absorbance at 273 nm, 278 nm and 280 nm wavelengths are used to semiquantify S lignin monomers, hardwood lignin and G lignin monomers respectively (Sarkanen and Hergert 1971; Irbe *et al.* 2006; Koehler and Telewski 2006; Sandquist *et al.* 2015). Different colours represent the absorbance intensities at different wavelengths and this information can be used to visualise the distribution of different lignin monomers, as can be seen, for example, across the secondary cell wall for various fibre cells in a xylem cross-section in Fig. 2c (Irbe *et al.* 2006; Carrillo *et al.* 2008). Similarly, UMSP can also reveal the subcellular distribution of phenolic extractives (Koch and Kleist 2001; Carrillo *et al.* 2008). Although the instrument that can perform UMSP is, not readily available, UMSP is a useful microanalytical technique both for qualitative and semi-quantitative chemotyping of secondary xylem.

X-ray photoelectron spectroscopy (XPS)

XPS can be used for both qualitative and semi-quantitative assessment of secondary xylem. Microtome sectioning is the only sample preparation step required, and samples with thicknesses in the millimetre or micrometre range are used. XPS is used to analyse cell wall structure and chemical composition and to semi-quantify cell wall polymers such as cellulose, hemicellulose and lignin, by analysing X-ray photoelectron spectra (Fig. 3a) (Sinn *et al.* 2001; Foston *et al.* 2011; Zuo *et al.* 2012; Banuls-Ciscar *et al.* 2016). Contemporary XPS analyses have the potential to provide both transverse and longitudinal (depth)

distribution information for chemotyping (Zuo *et al.* 2012). In addition to information about cell wall polymer distribution, XPS also detects extractives and inorganic elements such as calcium, potassium, phosphorus, nitrogen, carbon and oxygen (Shchukarev *et al.* 2002; Inari *et al.* 2006; Zuo *et al.* 2012; Banuls-Ciscar *et al.* 2016). Analysis of resulting spectral data provide qualitative information such as chemical structures and chemical bonds, and quantitative information such as changes in molecular concentrations (Foston *et al.* 2011; Zuo *et al.* 2012). According to Inari *et al*. (2006), results produced by XPS are in good agreement with those acquired by other spectroscopic methods. Therefore, XPS is an applicable, complementary, reliable method for chemotyping secondary xylem, and it delivers reproducible results.

Gas chromatography (GC) techniques

GC is a well-known and widely used micro chemotyping technique for identification and quantification of individual compounds in a mixture, usually in the form of an extraction. After preparation (see section 1), the sample is introduced to the GC set-up, where a carrier gas conveys the sample molecules to the injector port which volatilises the sample and introduces/injects it to the column for subsequent separation of sample components. Since the temperature of the injection port generally varies between 200 - 300°C, GC techniques are only informative for the compounds that can be vaporised below 300°C without decomposing. This limitation of GC techniques can be overcome by increasing the number of detectable compounds, through derivatising the sample to increase the volatility of polar fragments. However, this increases the labour-intensiveness of the sample preparation process. For quantification of monomers of cell wall polysaccharides (e.g. carbohydrates such as glucose, xylose) usually a dry weight of about 70 - 100 µg of cell wall material is used for the derivatisation-based sample preparation process (Angeles *et al.* 2006; MacMillan *et al.* 2015). After sample processing, as little as 1 µl of the processed sample can be injected into a capillary column (Biermann and McGinnis 1989).

GC can be coupled with one or more other instruments such as an autosampler, Mass Spectrometer (MS), Flame Ionisation Detector (FID) or pyrolyser, to reduce sample size and to enhance throughput, resolving power, compound detection sensitivity and data quality (Gerber *et al.* 2012; Al-Haddad *et al.* 2013; Lourenço *et al.* 2013). The use of an autosampler improves the throughput as it substitutes for slower manual injection of samples, and some autosamplers can even perform automated derivatisation of the sample. Coupling GC to MS (GC-MS) enables compound separation, identification and quantification of for example, different cell wall-derived monosaccharides such as arabinose, xylose, mannose, galactose and glucose (Angeles *et al.* 2006). When the objective is to analyse organic material, FID is the detector of choice. One common application of the Gas Chromatography/Flame Ionisation Detector (GC/FID) method is the analysis of monosaccharide compositions and lignin monomer ratios. GC analysis requires the construction of calibration curves for each monosaccharide (standard curves from pure monosaccharides), while for monosaccharides for which calibration samples are unavailable, the detector response of a suitable calibration sample is used to construct the calibration curve (Al-Haddad *et al.* 2013; Gerber *et al.* 2014).

Pyrolizers can thermally decompose material at high temperatures. Thus, when a pyrolizer is coupled to GC, labour-intensive sample preparation steps like extraction and hydrolysis become unnecessary, making Pyrolysis-Gas Chromatography (Py-GC), a convenient and high throughput method. Pyrolizers can also be coupled to techniques such as GC-MS and GC-FID, resulting in Pyrolysis-Gas Chromatography/Mass Spectrometry (Py-GC/MS) and Pyrolysis-Gas Chromatography/Flame Ionisation Detection (Py-GC/FID).

Pyrolysis requires only a small amount of sample (1 - 40 μg) either in the form of a ball-milled powder or as a thin tissue section (Lourenço *et al*. 2013; Gerber *et al*. 2014, 2016). Pyrolysis brings two significant advantages; pyrolytic reactions are applied to cell wall polymers in their *in-situ* context without any chemical separation or chemical modification, and it allows quantification of polysaccharides and lignin. Compared to Klason and acid-soluble lignin quantification methods (standard wet chemistry analytical methods for lignin), Py-GC/FID is more advantageous for evaluation of total lignin in particular since it accurately takes acid-soluble lignin into account (Lourenço *et al.* 2013). The chemotypic data generated from Py-GC/MS can be used either to semi-quantify cell wall polymers such as cellulose, hemicellulose and lignin or to fingerprint the sample. These data can also be used to obtain detailed information such as S, G and H lignin ratios (Lourenço *et al*. 2013, 2016; Lupoi *et al*. 2015; Gerber *et al*. 2016). Although Py-GC/MS is convenient in terms of sample preparation, the resulting chromatograms are complex due to the wide range and variety of decomposition products that can be formed (Fig. 3b). Several MS libraries are available via National Institute of Standards and Technology (NIST), to assist in the identification of these decomposed compounds. Overall, Py-GC/MS and Py-GC/FID provide high throughput and sensitive microanalytical techniques for chemotyping cell wall polymers in secondary xylem.

Fourier-transform infrared (FT-IR) spectroscopy

FTIR is a simple, convenient and non-destructive method to obtain structural and chemical fingerprints of cell walls. Chemotyping can be extended to detect conformational changes and putative cross-links between cell wall polymers (McCann *et al.* 1992; Alonso-Simón *et al.* 2011; Ohman *et al.* 2013). It uses an infrared (IR) beam to obtain a spectrum of absorption or emission of the samples. Wood samples can either be cryo-sectioned (~ 20 μm thickness) and then dried or ground depending on the FT-IR instrument being used. Ground samples can be placed directly into the IR beam, whereas the chemistry of secondary xylem sections can be mapped with a microscope (microspectroscopy) which has the potential to analyse areas as small as 50 × 50 μm effectively. Contemporary instruments in transmission mode can provide chemical fingerprints of cell walls with spatial resolutions in the 5 - 20 μm range (influenced by the wavelength of the radiation) (Lasch and Naumann 2006; Gorzsas *et al.* 2011). Smaller areas require an IR source that possesses a high brilliance (synchrotron), however, this might prove time-consuming and challenging (Gou *et al.* 2008). Several studies have provided detailed information on different FT-IR wavelengths assigned to different cell wall polymers including cellulose, lignin and hemicelluloses (Fig. 2d) (Müller and Polle 2009; Alonso-Simón *et al.* 2011; Gorzsas *et al.* 2011; Derba-Maceluch *et al.* 2015; Dai *et al.* 2020). In addition, near-infrared (FT-NIR) spectroscopy facilitates rapid determination of wood extractives and phenolic content in heartwood (Gierlinger *et al.* 2002). The use of multi-variate data analysis enables FT-IR to elucidate patterns of lignin composition in wood fibres which could not be detected by traditional data analysis (chemical imaging by heat mapping) (Gorzsas *et al.* 2011). However, FT-IR spectroscopy is only capable of semi-quantification since absolute quantification would require internal standards which at this stage are not available for this type of tissue analysis.

Matrix-assisted laser desorption ionisation mass spectrometry (MALDI-MS)

MALDI-MS is an ionisation method where the sample is mixed or coated with an energy-absorbing matrix such as silica to support the ionisation process. When a laser beam hits a target on the sample within the matrix, desorption and ionisation generate ions from the sample which can then be detected by a mass analyser such as MS (Liu *et al.* 2007; Lunsford *et al.* 2011; Araujo *et al.* 2014; Singhal *et al.* 2015). Sample preparation for MALDI-MS

typically involves sectioning, drying and spraying the matrix onto the sections (Araujo *et al.* 2014; Yoshinaga *et al.* 2016). Through combination with sophisticated equipment (e.g. LTQ-Orbitrap MS, Time-Of-Flight (TOF) analyser) and by altering laser optics, MALDI can be extended to single cell level chemotyping of cell wall polymers at a high resolution (ranging from 5 μm - few mm) (Obel *et al.* 2009; Araujo *et al.* 2014; Li *et al.* 2016; Feenstra *et al.* 2017; Qin *et al.* 2018). The resulting techniques, such as MALDI-TOF-MS, are high throughput microanalytical techniques for obtaining chemical fingerprints of cell walls (Fig. 2e) using wood samples as small as 100 ng (Persson *et al.* 2010; Bauer 2012; Boughton *et al.* 2016; Sturtevant *et al.* 2016). MALDI-MS can also determine S to G lignin ratios, and it also has the potential to provide semi quantitative information about some extractives such as terpenes (Sturtevant *et al.* 2016). When MALDI-MS is coupled with Oligosaccharide Mass Profiling (OLIMP), semi-quantitative data on cell wall oligosaccharides can be obtained from samples of around 1 μg (Obel *et al.* 2009; Persson *et al.* 2010). MALDI permits quantification only if a library of MS/MS data is available or if a calibration curve has been created. However, if such information is unavailable, the literature on ion fragmentation data (MS/MS) can be used (Araujo *et al.* 2014). MALDI methods serve as valuable microanalytical techniques for micro chemotyping secondary xylem.

Although micro chemotyping methods have many similarities among them in terms of requirements, restrictions and potentials, there are slight differences which make them unique. GC-based micro chemotyping methods can only identify cell wall polymers and provide quantitative information; however, these methods fail to demonstrate the distribution of cell wall polymers. In contrast, other techniques like XPS, FT-IR, MALDI-MS and UMSP can provide information which is both quantitative and qualitative (able to identify the cell wall polymers and to demonstrate their distribution on cell walls). Although XPS can perform optical sectioning and reveal information about subsurface structures (< 5 nm), it cannot achieve single cell resolution, which can be achieved by techniques such as FT-IR and MALDI-MS. A further comparison between these micro chemotyping techniques and an extensive summary are given in Table 5. Fig. 4 provides a decision guide to help the selection of a suitable micro chemotyping method based on some of the properties discussed in Table 5.

Dual micro morphotyping and chemotyping techniques

Microanalytical techniques discussed in this section have the capacity to perform aspects of both morphotyping and phenotyping, allowing data on both tissue/cell morphology and chemical composition to be obtained from a single technique.

Light microscopy (LM)

Light microscopy is inarguably the mainstay of phenotyping techniques, as it provides a straightforward method for both morphotyping and chemotyping. It uses thin sample sections (~ 1 - 30 μm thickness), which are prepared by either hand or microtome sectioning before being mounted on glass slides. Morphotyping can be done either with or without staining, at magnifications between 40× - 1000×, to view cellular features such as size, diameter, lumen size, microfibril angle, cell wall thickness and cell wall area. However, stained secondary xylem sections are often required for chemotyping as it helps to observe the presence or distribution patterns of cell wall polymers (Fig. 2f) (Sato *et al.* 2001; Wu *et al.* 2009; MacMillan *et al.* 2010; Manabe *et al.* 2013; Yang *et al.* 2017). Some frequently used stains in LM are listed in Table 1. Micrographs obtained by LM can be further analysed using a range of computer software packages such as ImageJ, Fiji, BioImageXD, and Icy among others (Eliceiri *et al.* 2012). LM has for example successfully revealed changes to wood cell

morphology and chemical composition in response to changing environmental conditions or tree genetics (Carrillo *et al.* 2008; Bao *et al.* 2012; Begum *et al.* 2012; Chai *et al.* 2015; Groover 2016; Kanbayashi and Miyafuji 2016; Yang *et al.* 2017). Compared to other advanced microscopy techniques, LM is inexpensive, sample preparation is relatively simple (if fixation/embedding are not required), it does not require much expertise, provides a method for visualising both live and dead cells and, if unstained, provides a means for observing a sample's natural colour. However, two main drawbacks of LM are low resolution (upper limit ~ 250 nm) and comparatively low magnification (upper limit ~ 1000×).

Fluorescence microscopy

Fluorescence is a type of LM that utilizes the fluorescence properties of the native sample or such properties introduced to a sample by fluorescent labels/stains, for visualisation of cell walls and cell wall polymers. Some of the most frequently used fluorescent stains are listed in Table 2. Lignin autofluorescence facilitates identification and visualisation of lignified cell walls and can be used to semi-quantify lignin between different cells, between distinct cell wall layers and different regions of the cell wall (Ma *et al.* 2013a). Cellulose in cell walls can be visualised by staining with calcofluor white which is one of the most commonly used fluorescent stains (Sato *et al.* 2001; Mitra and Loque 2014; Chai *et al.* 2015). In addition, FM is often employed to screen compression and normal wood (Donaldson *et al*. 2010, 2015; Donaldson and Knox 2012; Donaldson and Singh 2016). As an example, FM can be used to quantify the severity of compression wood using the ratio between the fluorescence produced at blue and violet wavelengths (Donaldson *et al.* 2010). Furthermore, FM is frequently used in immunohistochemistry using fluorescently labelled antibodies or fluorescently labelled carbohydrate binding modules (McCartney *et al.* 2004; Yang *et al.* 2013). Sample preparation is often as simple as sectioning (~ 20 μm thickness) except in cases where a fluorescent stain is required in which case there are additional staining steps.

Confocal laser scanning microscopy (CLSM)

Confocal microscopy performs non-destructive optical sectioning (~ 0.5 μm thickness) which enables observation of a relatively thick specimen (50 - 200 μm) at various depths, precluding the need for fine manual sectioning (Minsky 1988; Taguchi *et al.* 2010; Thorn 2016; Dickson *et al.* 2017). It enables both surface observations as well as the construction of 3D structures by using computer software to stack optical sections to generate a projection image (Kitin *et al.* 2003). CLSM allows the re-use of samples and precludes the introduction of artefacts that could arise from uneven thickness of sections and manual stacking of a series of sections. CLSM is often employed to observe changes taking place in secondary tissue/cell morphology and chemical composition following chemical treatment and as a result of altering tree genetics and/or environmental conditions (Fig. 2g) (Liu *et al.* 2017; Kong *et al.* 2018). CLSM is also used to analyse stem sections stained with antibodies or carbohydrate binding modules (Bao *et al.* 2012). For example, CLSM has been used to observe Sitka spruce compression wood sections labelled with LM5 antibody which provided insights into the synthesis of (1→4)-β-galactan as an initial response to compression wood formation (Altaner *et al.* 2007). Similarly, using CLSM and various antibodies (Table 3) the spatial distribution of non-cellulosic polysaccharides including distinct xyloglucan, heteroxylan, galactoglucomannan, and pectin epitopes have been observed in the secondary xylem of *Pinus radiata* (Putoczki *et al.* 2008; Donaldson and Knox 2012). Therefore, CLSM can be used for both morphotyping and chemotyping (Knebel and Schnepf 1991; Donaldson *et al.* 1999; Bao *et al.* 2012; Liu *et al.* 2017; Miller and Johnson 2017).

Transmission electron microscopy (TEM)

TEM has the highest resolving power of any of the methods described in this review (Duchesne and Daniel 1999; Reza *et al.* 2015). It facilitates tomography (a method for computing 3D structural data from a series of 2D images obtained at different angles), imaging (2D images) and analysis of cell wall polymers (Ercius *et al.* 2015). TEM can be coupled with analytical methods like Electron Energy-Loss Spectrometry (EELS) and Energy Dispersive X-ray Spectroscopy (EDX or EDS), to characterise chemicals or to analyse elements of samples (Reza *et al.* 2015). However, the requirement of ultra-thin samples (nanometre thicknesses), tedious sample preparation and the possibility for radiation damage are significant drawbacks of TEM (Reza *et al.* 2015; Wang *et al.* 2015). Sample preparation often involves embedding, ultramicrotomy and staining using some of the stains mentioned under staining in section 1. TEM and advanced versions of TEM, such as TEM-EDX, facilitate chemotyping by demonstrating the distribution of different polymers such as hemicellulose, lignin and even different monomers of lignin in cell walls (Reza *et al.* 2015). Compared to SEM, TEM micrographs are a lot 'cleaner' due to the absence of cell wall artefacts that could be introduced by sectioning. Some typical applications of TEM include morphotyping different cell types such as xylem fibre, vessels, axial and ray parenchyma (Fig. 2h), providing insights into fine structural details such as pit membrane, resence/ thickness of different cell wall layers (S1, S2 and S3 layer), molecular structure of microfibrils, microfibril angle in different cell wall layers and different structures formed by microfibrils (e.g. bundles, aggregates) (Duchesne and Daniel 1999; Xu *et al*. 2004, 2006, 2009, 2011; Donaldson and Xu 2005; Wilson *et al*. 2005; Ma *et al*. 2013a; Reza *et al*. 2015; Wang *et al*. 2015). In addition, TEM can be used to visualise the distribution of immunogold-labelled lignin, cellulose, (1→4)-β-galactan, arabinogalactan proteins and heteroxylans and (1→3)-β-glucan in wood cell walls (Altaner *et al.* 2010; Ruel *et al.* 2012; Kim and Daniel 2014, 2017). Furthermore, lead citrate staining enables TEM to reveal the distribution of phenolic extractives such as tannins in the lumina and cell walls of xylem vessels, fibres and parenchyma cells (Streit and Fengel 1994) and potassium permanganate staining reveals the distribution of lignin where noticeable changes can be correlated to the degree of lignification in each cell wall layer (Lehringer *et al.* 2009). Reza *et al*. (2015) provide an excellent review of TEM, where more examples can be found on how TEM can be employed for morpho-typing and chemotyping.

Raman spectroscopy

Raman spectroscopy allows label-free, non-destructive and high-resolution imaging of plant tissues at sub micrometre levels (< 0.5 μm). It exploits vibrational characteristics of molecules by utilising a monochromatic light source (laser) to measure the shift in energy of scattered photons which resembles the vibrational energy of the functional group that it is interacted with (Agarwal 2006; Schmidt *et al.* 2010; Foston *et al.* 2011; Gierlinger *et al.* 2012; Ma *et al.* 2013b; Zhang *et al.* 2017). Sample preparation often involves hand sectioning or microtomy and may or may not involve an embedding step depending on the features of interest. Secondary xylem sections (~ 3 μm - 0.5 mm thickness) with intact cell walls and flat surfaces can be used for Raman imaging. Nevertheless, the sample impurities or lignin autofluorescence or both could lead to false fluorescence which could hamper the measure-ments or conceal the actual Raman spectra; however, lignin autofluorescence can be mitigated by selecting a suitable excitation wavelength (Gierlinger and Schwanninger 2007; Gierlinger *et al.* 2012; Zhang *et al.* 2017).

Several modifications have been made to Raman spectroscopy to address issues associated with fluorescence, long image acquisition times and to enhance sensitivity and resolution

further. Confocal Raman micro-spectroscopy is one such approach that combines confocal microscopy with Raman spectroscopy to improve resolution and reduce fluorescence (Agarwal 2006; Gierlinger *et al.* 2012; Ma *et al.* 2013a). Near Infrared-Fourier Transform (NIR-FT) Raman spectroscopy utilises lasers in the IR range instead of visible light and coupling it with Fourier transformation successfully addresses the issues caused by fluorescence (Gierlinger and Schwanninger 2007). Coherent Anti-Stokes Raman Spectroscopy (CARS) employs two laser beams instead of one, resulting in reduced image acquisition times (Pohling *et al.* 2014). UV Resonance Raman Spectroscopy (UVRR) utilises lasers in the UV range thereby improving sensitivity. By introducing controlled microdisplacement (a microscopic movement) of the sample, this UVRR method can be extended to study single wood cells at the microscopic scale (Czaja *et al.* 2006). Specific band regions observed in the Raman spectrum can be used to assess and simultaneously map the distribution of cell wall polymers such as cellulose, lignin (S and G monomers), pectin and hemicellulose (Agarwal 2006; Gierlinger and Schwanninger 2006; Chu *et al.* 2010; Schmidt *et al.* 2010; Richter *et al.* 2011; Gierlinger *et al.* 2012; Ma *et al.* 2013b; Ozparpucu *et al.* 2017; Zhang *et al.* 2017). In addition, Raman spectroscopy also has the potential to reveal the cellular level distribution of wood extractives (Fig. 2i) (Belt *et al.* 2017). Band intensities in Raman spectroscopy are directly proportional to the analyte concentration, and therefore, semi-quantification can be achieved (Agarwal 2006). Raman spectroscopy is often used to assess cellular properties such as cell wall thickness, micromechanical properties of fibres (by analysing band shift patterns), microfibril angle, variability of cellulose microfibrils (at micron level) in different secondary cell wall layers and spatial distribution of carbohydrates (mainly cellulose) and lignin in cell walls (Gierlinger *et al.* 2010; Schmidt *et al.* 2010; Perera *et al.* 2012; Ma *et al.* 2013b). Hence, Raman spectroscopy serves as an efficient micro-analytical technique for morphotyping and chemotyping secondary xylem in its native state without the need for complex sample preparation.

Micro chemotyping techniques such as LM, CLSM, TEM and Raman spectroscopy can be used for both morphotyping and chemotyping. Although TEM and Raman spectroscopy provides both qualitative and quantitative information, LM and CLSM can only provide qualitative information. Compared to LM, CLSM has more properties such as optical sectioning, achieving single cell resolution and generation of 3D images. Raman spectroscopy also can achieve single cell resolution, and it can even reveal the micromechanical properties of the sample. Although TEM cannot reveal micromechanical properties, it can provide a resolution higher than that of any other dual micro morphotyping and chemotyping techniques.

CONCLUSIONS

Phenotyping of limited or small amounts of secondary xylem is challenging since only a few microanalytical techniques can successfully accommodate small samples. In this review, we aimed to provide a concise summary of some of the most commonly used microanalytical techniques highlighting their features, advantages and constraints in phenotyping secondary xylem. We have further simplified the task of selecting a suitable microanalytical technique by providing a comprehensive comparison and selection guide (Table 4, Table 5 and Fig. 4) between these microanalytical techniques based on eleven critical properties that need to be taken into consideration such as amount of sample/sample thickness, sample preparation, technical and labour demand, tissue/cellular integrity after sample preparation, possibility of sample damage during imaging/analysis, ability to reveal details on surface structures and beneath surface structures, and the qualitative/quantitative nature of the output. However, the ultimate selection of a suitable technique is at the user's discretion and depends on the scope

of the study, cost and resource availability.

ACKNOWLEDGEMENTS
We thank our colleagues (mentioned in Fig. 2 and 3) for providing permission to use their material. We gratefully acknowledge Barbara Ozarska for critically reading our manuscript. NK acknowledges Melbourne Research Scholarship (MRS) funding from The University of Melbourne.

REFERENCES
Agarwal UP. 2006. Raman imaging to investigate ultrastructure and composition of plant cell walls: distribution of lignin and cellulose in black spruce wood (*Picea mariana*). Planta. 224: 1141–1153. DOI:10.1007/s00425-006-0295-z.

Al-Haddad JM, Kang KY, Mansfield SD, Telewski FW. 2013. Chemical responses to modified lignin composition in tension wood of hybrid poplar (*Populus tremula* x *Populus alba*). Tree Physiol. 33: 365–373. DOI:10.1093/treephys/tpt017.

Alonso-Simón A, García-Angulo P, Mélida H, Encina A, Álvarez JM, Acebes JL. 2011. The use of FTIR spectroscopy to monitor modifications in plant cell wall architecture caused by cellulose biosynthesis inhibitors. Plant Signal Behav. 6: 1104–1110. DOI:10.4161/psb.6.8.15793.

Altaner C, Hapca AI, Knox JP, Jarvis MC. 2007. Detection of β-1-4-galactan in compression wood of Sitka spruce *Picea sitchensis* (Bong.) Carriere by immunofluorescence. Holzforschung. 61: 311–316. DOI:10.1515/hf.2007.049.

Altaner CM, Tokareva EN, Jarvis MC, Harris PJ. 2010. Distribution of (1→4)-beta-galactans, arabinogalactan proteins, xylans and (1→3)-beta-glucans in tracheid cell walls of softwoods. Tree Physiol. 30: 782–793. DOI:10.1093/treephys/tpq021.

Altartouri B, Bidhendi AJ, Tani T, Suzuki J, Conrad C, Chebli Y, Liu N, Karunakaran C, Scarcelli G, Geitmann A. 2019. Pectin chemistry and cellulose crystallinity govern pavement cell morphogenesis in a multi-step mechanism. Plant Physiol. 181: 127–141. DOI:10.1104/pp.19.00303.

Anderson CT, Carroll A, Akhmetova L, Somerville C. 2010. Real-time imaging of cellulose reorientation during cell wall expansion in *Arabidopsis* roots. Plant Physiol. 152: 787–796. DOI:10.1104/pp.109.150128.

Andersson-Gunneras S, Mellerowicz EJ, Love J, Segerman B, Ohmiya Y, Coutinho PM, Nilsson P, Henrissat B, Moritz T, Sundberg B. 2006. Biosynthesis of cellulose-enriched tension wood in *Populus*: global analysis of transcripts and metabolites identifies biochemical and developmental regulators in secondary wall biosynthesis. Plant J. 45: 144–165. DOI:10.1111/j.1365-313X.2005.02584.x.

Andersson S, Serimaa R, Torkkeli M, Paakkari T, Saranpää P, Pesonen E. 2000. Microfibril angle of Norway spruce *Picea abies* (L.) Karst. compression wood: comparison of measuring techniques. J. Wood Sci. 46: 343–349. DOI:10.1007/BF00776394.

Angeles G, Berrio-Sierra J, Joseleau JP, Lorimier P, Lefebvre A, Ruel K. 2006. Preparative laser capture microdissection and single-pot cell wall material preparation: a novel method for tissue-specific analysis. Planta. 224: 228–232. DOI:10.1007/s00425-006-0285-1.

Araujo P, Ferreira MS, de Oliyeira DN, Pereira L, Sawaya A, Catharino RR, Mazzafera P. 2014. Mass spectrometry imaging: an expeditious and powerful technique for fast in situ lignin assessment in *Eucalyptus*. Anal. Chem. 86: 3415–3419. DOI:10.1021/ac500220r.

Arend M. 2008. Immunolocalization of (1,4)-β-galactan in tension wood fibers of poplar. Tree Physiol. 28: 1263–1267. DOI:10.1093/treephys/28.8.1263.

Ariel P. 2017. A beginner's guide to tissue clearing. Int. J. Biochem. Cell Biol. 84: 35–39. DOI: 10.1016/j.bioce1.2016.12.009.

Bañuls-Ciscar J, Pratelli D, Abel ML, Watts JF. 2016. Surface characterisation of pine wood by XPS. Surf. Interface Anal. 48: 589–592. DOI:10.1002/sia.5960.

Bao CC, Wang J, Zhang RH, Zhang BC, Zhang H, Zhou YH, Huang SJ. 2012. *Arabidopsis* VILLIN2 and VILLIN3 act redundantly in sclerenchyma development via bundling of actin filaments. Plant J. 71: 962–975. DOI:10.1111/j.1365-313X.2012.05044.x.

Bauer S. 2012. Mass spectrometry for characterizing plant cell wall polysaccharides. Front. Plant Sci. 3: 1–6. DOI:10.3389/fpls.2012.00045.

Begum S, Nakaba S, Yamagishi Y, Yamane K, Islam A, Oribe Y, Ko JH, Jin HO, Funada R. 2012. A rapid decrease in temperature induces latewood formation in artificially reactivated cambium of conifer stems. Ann. Bot. 110: 875–885. DOI:10.1093/aob/mcs149.

Belt T, Keplinger T, Hanninen T, Rautkari L. 2017. Cellular level distributions of Scots pine heartwood and knot heartwood extractives revealed by Raman spectroscopy imaging. Ind. Crops Prod. 108: 327–335. DOI:10.1016/j.indcrop.2017.06.056.

Biermann CJ, McGinnis GD. 1989. Analysis of carbohydrates by GLC and MS. CRC press, Boca Raton, FL, USA.

Blake AW, McCartney L, Flint JE, Bolam DN, Boraston AB, Gilbert HJ, Knox JP. 2006. Understanding the biological rationale for the diversity of cellulose-directed carbohydrate-binding modules in prokaryotic enzymes. J. Biol. Chem. 281: 29321–29329. DOI:10.1074/jbc.M605903200.

Bond J, Donaldson L, Hill S, Hitchcock K. 2008. Safranine fluorescent staining of wood cell walls. Biotech. Histochem. 83: 161–171. DOI:10.1080/10520290802373354.

Borgin K, Parameswaran N, Liese W. 1975. The effect of aging on the ultrastructure of wood. Wood Sci. Technol. 9: 87–98. DOI:10.1007/bf00353388.

Boughton BA, Thinagaran D, Sarabia D, Bacic A, Roessner U. 2016. Mass spectrometry imaging for plant biology: a review. Phytochem. Rev. 15: 445–488. DOI:10.1007/s11101-015-9440-2.

Brodersen CR. 2013. Visualizing wood anatomy in three dimensions with high-resolution x-ray micro-tomography (μCT) - a review. IAWA J. 34: 408–424. DOI:10.1163/22941932-00000033.

Brundrett MC, Enstone DE, Peterson CA. 1988. A berberine-aniline blue fluorescent staining procedure for suberin, lignin, and callose in plant tissue. Protoplasma. 146: 133–142. DOI:10.1007/BF01405922.

Brundrett MC, Kendrick B, Peterson CA. 1991. Efficient lipid staining in plant material with sudan red 7B or fluoral yellow 088 in polyethylene glycol-glycerol. Biotech. Histochem. 66: 111–116. DOI:10.3109/10520299109110562.

Carrillo A, Mayer I, Koch G, Hapla F. 2008. Wood anatomical characteristics and chemical composition of *Prosopis laevigata* grown in the Northeast of Mexico. IAWA J. 29: 25–34. DOI:10.1163/22941932-90000167.

Chaffey N, Cholewa E, Regan S, Sundberg B. 2002. Secondary xylem development in *Arabidopsis*: a model for wood formation. Physiol. Plant. 114: 594–600. DOI: 10.1034/j.1399-3054.2002.1140413.x.

Chai GH, Kong YZ, Zhu M, Yu L, Qi G, Tang XF, Wang ZG, Cao YP, Yu CJ, Zhou GK. 2015. *Arabidopsis* C3H14 and C3H15 have overlapping roles in the regulation of secondary wall thickening and anther development. J. Exp. Bot. 66: 2595–2609. DOI: 10.1093/jxb/erv060.

Chu LQ, Masyuko R, Sweedler JV, Bohn PW. 2010. Base-induced delignification of *Miscanthus* x *giganteus* studied by three-dimensional confocal Raman imaging. Bioresource Technol. 101: 4919–4925. DOI: 10.1016/j.biortech.2009.10.096.

Clausen MH, Willats WGT, Knox JP. 2003. Synthetic methyl hexagalacturonate hapten inhibitors of antihomogalacturonan monoclonal antibodies LM7, JIM5 and JIM7. Carbohydr. Res. 338: 1797–1800. DOI:10.1016/s0008-6215(03)00272-6.

Czaja AD, Kudryavtsev AB, Schopf JW. 2006. New method for the microscopic, non-destructive acquisition of ultraviolet resonance Raman spectra from plant cell walls. Appl. Spectrosc. 60: 352–355. DOI:10.1366/000370206776593753.

Dai Y, Hu G, Dupas A, Medina L, Blandels N, *et al*. 2020. Implementing the CRISPR/Cas9 technology in *Eucalyptus* hairy roots using wood-related genes. Int. J. Mol. Sci. 21: 3408. DOI:10.3390/ijms21103408.

Dejardin A, Laurans F, Arnaud D, Breton C, Pilate G, Leplé JC. 2010. Wood formation in angiosperms. C.R. Biol. 333: 325–334. DOI: 10.1016/j.crvi.2010.01.010.

Derba-Maceluch M, Awano T, Takahashi J, Lucenius J, Ratke C, *et al*. 2015. Suppression of

xylan endotransglycosylase PtxtXyn10A affects cellulose microfibril angle in secondary wall in aspen wood. New Phytol. 205: 666–681. DOI:10.1111/nph.13099.

Dickson A, Nanayakkara B, Sellier D, Meason D, Donaldson L, Brownlie R. 2017. Fluorescence imaging of cambial zones to study wood formation in *Pinus radiata* D. Don. Trees. 31: 479–490. DOI:10.1007/s00468-016-1469-3.

Dogu AD, Grabner M. 2010. A staining method for determining severity of tension wood. Turk J Agric For. 34: 381–392. DOI:10.3906/tar-0906-209.

Donaldson L, Bardage S, Daniel G. 2007. Three-dimensional imaging of a sawn surface: a comparison of confocal microscopy, scanning electron microscopy, and light microscopy combined with serial sectioning. Wood Sci. Technol. 41: 551–564. DOI: 10.1007/s00226-007-0132-y.

Donaldson L, Radotić K, Kalauzi A, Djikanović D, Jeremić M. 2010. Quantification of compression wood severity in tracheids of *Pinus radiata* D. Don using confocal fluorescence imaging and spectral deconvolution. J. Struct. Biol. 169: 106–115. DOI: 10.1016/j.jsb.2009.09.006.

Donaldson L, Xu P. 2005. Microfibril orientation across the secondary cell wall of Radiata pine tracheids. Trees. 19: 644–653. DOI: 10.1007/s00468-005-0428-1.

Donaldson LA. 2019. Wood cell wall ultrastructure: The key to understanding wood properties and behaviour. IAWA J. 40: 645–672. DOI:10.1163/22941932-40190258.

Donaldson LA, Knox JP. 2012. Localization of cell wall polysaccharides in normal and compression wood of radiata pine: relationships with lignification and microfibril orientation. Plant Physiol. 158: 642–653. DOI:10.1104/pp.111.184036.

Donaldson LA, Nanayakkara B, Radotić K, Djikanović-Golubović D, Mitrović A, Pristov JB, Radosavljević JS, Kalauzi A. 2015. Xylem parenchyma cell walls lack a gravitropic response in conifer compression wood. Planta. 242: 1413–1424. DOI:10.1007/s00425-015-2381-6.

Donaldson LA, Singh AP. 2016. Reaction wood. In: YS Kim, R Funada, AP Singh (eds), Secondary xylem biology: 93–110. Academic Press, Boston, USA.

Donaldson LA, Singh AP, Yoshinaga A, Takabe K. 1999. Lignin distribution in mild compression wood of *Pinus radiata*. Can. J. Bot. 77: 41–50. DOI:10.1139/b98-190.

Duchesne I, Daniel G. 1999. The ultrastructure of wood fibre surfaces as shown by a variety of microscopical methods - A review. Nord Pulp Pap. Res. J. 14: 129–139. DOI: 10.3183/npprj-1999-14-02-p129-139.

Eckert C, Sharmin S, Kogel A, Yu D, Kins L, Strijkstra GJ, Polle A. 2019. What makes the wood? Exploring the molecular mechanisms of xylem acclimation in hardwoods to an ever-changing environment. Forests. 10: 358. DOI:10.3390/f10040358.

Ehmcke G, Pilgard A, Koch G, Richter K. 2017. Topochemical analyses of furfuryl alcohol modified radiata pine (*Pinus radiata*) by UMSP, light microscopy and SEM. Holzforschung. 71: 821–831. DOI:10.1515/hf-2016-0219.

Eliceiri KW, Berthold MR, Goldberg IG, Ibanez L, Manjunath BS, *et al*. 2012. Biological imaging software tools. Nat. Methods. 9: 697–710. DOI:10.1038/nmeth.2084.

Ercius P, Alaidi O, Rames MJ, Ren G. 2015. Electron tomography: A three-dimensional analytic tool for hard and soft materials research. Adv. Mater. 27: 5638–5663. DOI: 10.1002/adma.201501015.

Evans R. 1994. Rapid measurement of the transverse dimensions of tracheids in radial wood sections from *Pinus radiata*. Holzforschung. 48: 168–172. DOI:10.1515/hfsg.1994.48.2.168.

Evans R, Ilic J. 2001. Rapid prediction of wood stiffness from microfibril, angle and density. For. Prod. J. 51: 53–57.

Evans R, Stringer S, Kibblewhite RP. 2000. Variation of microfibril angle, density and fibre orientation in twenty-nine *Eucalyptus nitens* trees. Appita J. 53: 450–457.

Feenstra AD, Duenas ME, Lee YJ. 2017. Five-micron high resolution MALDI mass spectrometry imaging with simple, interchangeable, multi-resolution optical system. J. Am. Soc. Mass Spectrom. 28: 434–442. DOI:10.1007/s13361-016-1577-8.

Felten J, Vahala J, Love J, Gorzsás A, Ruggeberg M, et al. 2018. Ethylene signalling induces gelatinous layers with typical features of tension wood in hybrid aspen. New Phytol. 218: 999–1014. DOI:10.1111/nph.15078.

Filonova L, Kallas AM, Greffe L, Johansson G, Teeri TT, Daniel G. 2007. Analysis of the surfaces of wood tissues and pulp fibers using carbohydrate-binding modules specific for crystalline cellulose and mannan. Biomacromolecules. 8: 91–97. DOI: 10.1021/bm060632z.

Foston M, Hubbell CA, Samuel R, Jung S, Fan H, *et al*. 2011. Chemical, ultrastructural and supramolecular analysis of tension wood in *Populus tremula* x *alba* as a model substrate for reduced recalcitrance. Energy Environ. Sci. 4: 4962–4971. DOI:10.1039/c1ee02073k.

Fukazawa K. 1992. Ultraviolet microscopy. In: SY Lin, CW Dence (eds), Methods in lignin chemistry: 110–121. Springer-Verlag, Berlin, Heidelberg.

Gerber L, Eliasson M, Trygg J, Moritz T, Sundberg B. 2012. Multivariate curve resolution provides a high-throughput data processing pipeline for pyrolysis-gas chromatography/mass spectrometry. J. Anal. Appl. Pyrolysis. 95: 95–100. DOI: 10.1016/j.jaap.2012.01.011.

Gerber L, Ohman D, Kumar M, Ranocha P, Goffner D, Sundberg B. 2016. High-throughput

microanalysis of large lignocellulosic sample sets by pyrolysis-gas chromatography/mass spectrometry. Physiol. Plant. 156: 127–138. DOI: 10.1111/ppl.12397.

Gerber L, Zhang B, Roach M, Rende U, Gorzsás A, Kumar M, Burgert I, Niittyla T, Sundberg B. 2014. Deficient sucrose synthase activity in developing wood does not specifically affect cellulose biosynthesis but causes an overall decrease in cell wall polymers. New Phytol. 203: 1220–1230. DOI:10.1111/nph.12888.

Gierlinger N, Keplinger T, Harrington M. 2012. Imaging of plant cell walls by confocal Raman microscopy. Nat. Protoc. 7: 1694–1708. DOI:10.1038/nprot.2012.092.

Gierlinger N, Luss S, Konig C, Konnerth J, Eder M, Fratzl P. 2010. Cellulose microfibril orientation of *Picea abies* and its variability at the micron-level determined by Raman imaging. J. Exp. Bot. 61: 587–595. DOI:10.1093/jxb/erp325.

Gierlinger N, Schwanninger M. 2006. Chemical imaging of poplar wood cell walls by confocal Raman microscopy. Plant Physiol. 140: 1246–1254. DOI:10.1104/pp.105.066993.

Gierlinger N, Schwanninger M. 2007. The potential of Raman microscopy and Raman imaging in plant research. Spectroscopy. 21: 69–89. DOI:10.1155/2007/498206.

Gierlinger N, Schwanninger M, Hinterstoisser B, Wimmer R. 2002. Rapid determination of heartwood extractives in *Larix* sp by means of Fourier transform near infrared spectroscopy. J. Near Infrared Spectrosc. 10: 203–214. DOI:10.1255/jnirs.336.

Gorzsás A, Stenlund H, Persson P, Trygg J, Sundberg B. 2011. Cell-specific chemotyping and multivariate imaging by combined FT-IR microspectroscopy and orthogonal projections to latent structures (OPLS) analysis reveals the chemical landscape of secondary xylem. Plant J. 66: 903–914. DOI:10.1111/j.1365-313X.2011.04542.x.

Gou JY, Park S, Yu XH, Miller LM, Liu CJ. 2008. Compositional characterization and imaging of "wall-bound" acylesters of *Populus trichocarpa* reveal differential accumulation of acyl molecules in normal and reactive woods. Planta. 229: 15–24. DOI: 10.1007/s00425-008-0799-9.

Gray JD, Kolesik P, Hoj PB, Coombe BG. 1999. Confocal measurement of the three-dimensional size and shape of plant parenchyma cells in a developing fruit tissue. Plant J. 19: 229–236. DOI:10.1046/j.1365-313X.1999.00512.x.

Gritsch C, Wan YF, Mitchell RAC, Shewry PR, Hanley SJ, Karp A. 2015. G-fibre cell wall development in willow stems during tension wood induction. J. Exp. Bot. 66: 6447–6459. DOI:10.1093/jxb/erv358.

Groover A. 2016. Gravitropisms and reaction woods of forest trees - evolution, functions and mechanisms. New Phytol. 211: 790–802. DOI:10.1111/nph.13968.

Groover A, Robischon M. 2006. Developmental mechanisms regulating secondary growth in woody plants. Curr. Opin. Plant Biol. 9: 55–58. DOI: 10.1016/j.pbi.2005.11.013.

Hayat D. 2002. Microscopy, immunohistochemistry, and antigen retrieval methods. Springer, USA.

Hepler PK, Newcomb EH. 1963. Fine structure of young tracheary xylem elements arising by redifferentiation of parenchyma in wounded coleus stem. J. Exp. Bot. 14: 496–503. DOI:10.1093/jxb/14.3.496.

Heu R, Shahbazmohamadi S, Yorston J, Capeder P. 2019. Target material selection for sputter coating of SEM samples. Microscopy Today. 27: 32–36. DOI:10.1017/S1551929519000610.

Hilden L, Daniel G, Johansson G. 2003. Use of a fluorescence labelled, carbohydrate-binding module from *Phanerochaete chrysosporium* Cel7D for studying wood cell wall ultrastructure. Biotechnol. Lett. 25: 553–558. DOI:10.1023/a:1022846304826.

Hubbe MA, Chandra RP, Dogu D, van Velzen STJ. 2019. Analytical staining of cellulosic materials: a review. Bioresources. 14: 7387–7464.

Inari GN, Petrissans M, Lambert J, Ehrhardt JJ, Gerardin P. 2006. XPS characterization of wood chemical composition after heat-treatment. Surf. Interface Anal. 38: 1336–1342. DOI:10.1002/sia.2455.

Irbe I, Noldt G, Koch G, Andersone I, Andersons B. 2006. Application of scanning UV microspectrophotometry for the topochemical detection of lignin within individual cell walls of brown-rotted Scots pine (*Pinus sylvestris* L.) sapwood. Holzforschung. 60: 601–607. DOI:10.1515/hf2006.102.

Jacquin P, Longuetaud F, Leban JM, Mothe F. 2017. X-ray microdensitometry of wood: a review of existing principles and devices. Dendrochronologia. 42: 42–50. DOI: 10.1016/j.dendro.2017.01.004.

Kanbayashi T, Miyafuji H. 2016. Effect of ionic liquid treatment on the ultrastructural and topochemical features of compression wood in Japanese cedar (*Cryptomeria japonica*). Sci. Rep. 6: 30147. DOI:10.1038/srep30147.

Kidner C, Groover A, Thomas DC, Emelianova K, Soliz-Gamboa C, Lens F. 2016. First steps in studying the origins of secondary woodiness in *Begonia* (Begoniaceae): combining anatomy, phylogenetics, and stem transcriptomics. Biol. J. Linn. Soc. 117: 121–138. DOI:10.1111/bij.12492.

Kim JS, Daniel G. 2014. Immunocytochemical studies of axial resin canals. I. Localization of non-cellulosic polysaccharides in epithelium of Norway spruce xylem. IAWA J. 35: 236–252. DOI: 10.1163/22941932-00000063.

Kim JS, Daniel G. 2017. Immunolocalization of pectin and hemicellulose epitopes in the phloem of Norway spruce and Scots pine. Trees. 31: 1335–1353. DOI:10.1007/s00468-017-1552-4.

Kitin P, Funada R, Sano Y, Ohtani J. 2000. Analysis by confocal microscopy of the structure of cambium in the hardwood *Kalopanax pictus*. Ann. Bot. 86: 1109–1117. DOI:10.1006/anbo.2000.1281.

Kitin P, Sano Y, Funada R. 2002. Fusiform cells in the cambium of *Kalopanax pictus* are exclusively mononucleate. J. Exp. Bot. 53: 483–488. DOI:10.1093/jexbot/53.368.483.

Kitin P, Sano Y, Funada R. 2003. Three-dimensional imaging and analysis of differentiating secondary xylem by confocal microscopy. IAWA J. 24: 211–222. DOI:10.1163/22941932-90001590.

Knebel W, Schnepf E. 1991. Confocal laser scanning microscopy of fluorescently stained wood cells - a new method for 3-dimensional imaging of xylem elements. Trees. 5: 1–4. DOI:10.1007/BF00225328.

Knox JP. 1997. The use of antibodies to study the architecture and developmental regulation of plant cell walls. Int. Rev. Cytol. 171: 79–120.

Knox JP. 2008. Revealing the structural and functional diversity of plant cell walls. Curr. Opin. Plant Biol. 11: 308–313. DOI: 10.1016/j.pbi.2008.03.001.

Koch G, Grunwald C. 2004. Application of UV microspectrophotometry for the topochemical detection of lignin and phenolic extractives in wood fibre cell walls. In: U Schmitt (ed.), Wood fibre cell walls: Methods to study their formation, structure and properties: 119–130. Swedish University of Agricultural Sciences, Uppsala, Sweden.

Koch G, Kleist G. 2001. Application of scanning UV microspectrophotometry to localise lignins and phenolic extractives in plant cell walls. Holzforschung 55: 563–567. DOI: 10.1515/hf.2001.091.

Koehler L, Telewski FW. 2006. Biomechanics and transgenic wood. Am. J. Bot. 93: 1433–1438. DOI:10.3732/ajb.93.10.1433.

Kong LZ, Guan H, Wang XQ. 2018. In situ polymerization of furfuryl alcohol with ammonium dihydrogen phosphate in poplar wood for improved dimensional stability and flame retardancy. ACS Sustain. Chem. Eng. 6: 3349–3357. DOI:10.1021/acssuschemeng.7b03518.

Kraus JE, de Sousa HC, Rezende MH, Castro NM, Vecchi C, Luque R. 1998. Astra blue and basic fuchsin double staining of plant materials. Biotech. Histochem. 73: 235–243. DOI:10.3109/10520299809141117.

Lafarguette F, Leplé JC, Déjardin A, Laurans F, Costa G, Lesage-Descauses MC, Pilate G. 2004. Poplar genes encoding fasciclin-like arabinogalactan proteins are highly expressed in tension wood. New Phytol. 164: 107–121. DOI:10.1111/j.1469-8137.2004.01175.x.

Lasch P, Naumann D. 2006. Spatial resolution in infrared micro spectroscopic imaging of tissues. Biochim. Biophys. Acta. 1758: 814–829. DOI: 10.1016/j.bbamem.2006.06.008.

Lehringer C, Daniel G, Schmitt U. 2009. TEM/FE-SEM studies on tension wood fibres of *Acer* spp., *Fagus sylvatica* L. and *Quercus robur* L. Wood Sci. Technol. 43: 691–702. DOI:10.1007/s00226-009-0260-7.

Li B, Bhandari DR, Rompp A, Spengler B. 2016. High-resolution MALDI mass spectrometry imaging of gallotannins and monoterpene glucosides in the root of *Paeonia lactiflora*. Sci. Rep. 6: 36074. DOI:10.1038/srep36074.

Liebsch D, Sunaryo W, Holmlund M, Norberg M, Zhang J, *et al*. 2014. Class I KNOX transcription factors promote differentiation of cambial derivatives into xylem fibers in the *Arabidopsis* hypocotyl. Development. 141: 4311–4319. DOI:10.1242/dev.111369.

Lima JT, Ribeiro AD, Narciso CRP. 2014. Microfibril angle of *Eucalyptus grandis* wood in relation to the cambial age. Maderas-Cienc. Tecnol. 16: 487–494. DOI:10.4067/s0718-221x2014005000039.

Liu CW, Su ML, Zhou XW, Zhao RJ, Lu JX, Wang YR. 2017. Analysis of content and distribution of lignin in cell wall of transgenic poplar with Fourier Infrared Spectrum (FTIR) and Confocal Laser Scanning Microscopy (CLSM). Spectrosc. Spect. Anal. 37: 3404–3408. DOI: 10.3964/j.issn.1000-0593(2017)11-3404-05.

Liu LF, Shang-Guan KK, Zhang BC, Liu XL, Yan MX, *et al*. 2013. Brittle Culm1, a COBRA-like protein, functions in cellulose assembly through binding cellulose microfibrils. PLoS Genet. 9: e1003704. DOI: 10.1371/journal.pgen.1003704.

Liu Q, Guo Z, He L. 2007. Mass spectrometry imaging of small molecules using desorption/ionization on silicon. Anal. Chem. 79: 3535–3541. DOI: 10.1021/ac0611465.

Loqman MY, Bush PG, Farquharson C, Hall AC. 2010. A cell shrinkage artefact in growth plate chondrocytes with common fixative solutions: importance of fixative osmolarity for maintaining morphology. Eur. Cells Mater. 19: 214–227. DOI: 10.22203/eCM.v019a21.

Lourenço A, Gominho J, Marques AV, Pereira H. 2013. Comparison of Py-GC/FID and wet chemistry analysis for lignin determination in wood and pulps from *Eucalyptus globulus*. Bioresources. 8: 2967–2980.

Lourenço A, Rencoret J, Chemetova C, Gominho J, Gutiérrez A, del Río JC, Pereira H. 2016. Lignin composition and structure differs between xylem, phloem and phellem in *Quercus suber* L. Front. Plant Sci. 7: 1612. DOI:10.3389/fpls.2016.01612.

Lunsford KA, Peter GF, Yost RA. 2011. Direct matrix-assisted laser desorption/ionization mass spectrometric imaging of cellulose and hemicellulose in *Populus* tissue. Anal. Chem. 83: 6722–6730. DOI:10.1021/ac2013527.

Lupoi JS, Singh S, Parthasarathi R, Simmons BA, Henry RJ. 2015. Recent innovations in analytical methods for the qualitative and quantitative assessment of lignin. Renew. Sust. Energ. Rev. 49: 871–906. DOI: 10.1016/j.rser.2015.04.091.

Lux A, Morita S, Abe J, Ito K. 2005. An improved method for clearing and staining free-hand sections and whole-mount samples. Ann. Bot. 96: 989–996. DOI:10.1093/aob/mci266.

Ma JF, Ji Z, Zhou X, Zhang ZH, Xu F. 2013a. Transmission electron microscopy, fluorescence microscopy, and confocal Raman microscopic analysis of ultrastructural and compositional heterogeneity of *Cornus alba* L. wood cell wall. Microsc. Microanal. 19: 243–253. DOI:10.1017/s1431927612013906.

Ma JF, Zhou X, Zhang X, Xu F. 2013b. Label-free in situ Raman analysis of opposite and tension wood in *Populus nigra*. Bioresources. 8: 2222–2233.

MacMillan CP, Mansfield SD, Stachurski ZH, Evans R, Southerton SG. 2010. Fasciclin-like arabinogalactan proteins: specialization for stem biomechanics and cell wall architecture in *Arabidopsis* and *Eucalyptus*. Plant J. 62: 689–703. DOI:10.1111/j.1365-313X.2010.04181.x.

MacMillan CP, Taylor L, Bi YD, Southerton SG, Evans R, Spokevicius A. 2015. The fasciclin-like arabinogalactan protein family of *Eucalyptus grandis* contains members that impact wood biology and biomechanics. New Phytol. 206: 1314–1327. DOI:10.1111/nph.13320.

Mahesh S, Kumar P, Ansari SA. 2015. A rapid and economical method for the maceration of wood fibers in *Boswellia serrata* Roxb. Tropical Plant Research. 2: 108–111.

Maloney VJ, Mansfield SD. 2010. Characterization and varied expression of a membrane-bound endo-β-1,4-glucanase in hybrid poplar. Plant Biotechnol. J. 8: 294–307. DOI:10.1111/j.1467-7652.2009.00483.x.

Manabe Y, Verhertbruggen Y, Gille S, Harholt J, Chong SL, *et al*. 2013. Reduced wall acetylation proteins play vital and distinct roles in cell wall O-acetylation in *Arabidopsis*. Plant Physiol. 163: 1107–1117. DOI:10.1104/pp.113.225193.

Mayo SC, Chen F, Evans R. 2010. Micron-scale 3D imaging of wood and plant microstructure using high-resolution X-ray phase-contrast microtomography. J. Struct. Biol. 171: 182–188. DOI: 10.1016/j.jsb.2010.04.001.

McCann MC, Hammouri M, Wilson R, Belton P, Roberts K. 1992. Fourier transform infrared microspectroscopy is a new way to look at plant cell walls. Plant Physiol. 100: 1940–1947. DOI:10.1104/pp.100.4.1940.

McCartney L, Gilbert HJ, Bolam DN, Boraston AB, Knox JP. 2004. Glycoside hydrolase carbohydrate-binding modules as molecular probes for the analysis of plant cell wall polymers. Anal. Biochem. 326: 49–54. DOI:10.1016/j.ab.2003.11.011.

Meikle PJ, Bonig I, Hoogenraad NJ, Clarke AE, Stone BA. 1991. The location of (1- 3)-β-glucans in the walls of pollen tubes of pollen tubes of *Nicotiana alata* using (1- 3)-β-glucan-specific monoclonal antibody. Planta 185: 1–8.

Melder E, Bossinger G, Spokevicius AV. 2015. Overexpression of ARBORKNOX1 delays the differentiation of induced somatic sector analysis (ISSA) derived xylem fibre cells in poplar stems. Tree Genet. Genom. 11: 87. DOI:10.1007/s11295-015-0912-8.

Miller ML, Johnson DM. 2017. Vascular development in very young conifer seedlings: Theoretical hydraulic capacities and potential resistance to embolism. Am. J. Bot. 104: 979–992. DOI:10.3732/ajb.1700161.

Minsky M. 1988. Memoir on inventing the confocal scanning microscope. Scanning 10: 128−138. DOI:10.1002/sca.4950100403.

Mitra PP, Loque D. 2014. Histochemical staining of *Arabidopsis thaliana* secondary cell wall elements. J. Vis. Exp. 87: e51381. DOI:10.3791/51381.

Möller R, Koch G, Nanayakkara B, Schmitt U. 2006. Lignification in cell cultures of *Pinus radiata*: activities of enzymes and lignin topochemistry. Tree Physiol. 26: 201−210. DOI:10.1093/treephys/26.2.201.

Morris H, Plavcova L, Gorai M, Klepsch MM, Kotowska M, Schenk HJ, Jansen S. 2018. Vessel-associated cells in angiosperm xylem: highly specialized living cells at the symplast-apoplast boundary. Am. J. Bot. 105: 151−160. DOI:10.1002/ajb2.1030.

Müller G, Polle A. 2009. Imaging of lignin and cellulose in hardwood using fourier transform infrared microscopy – comparison of two methods. NZ. J. For. Sci. 39: 225−231.

Obel N, Erben V, Schwarz T, Kuhnel S, Fodor A, Pauly M. 2009. Microanalysis of plant cell wall polysaccharides. Mol. Plant 2: 922−932. DOI:10.1093/mp/ssp046.

Øbro J, Sørensen T, Möller I, Skjøt M, Mikkelsen JD, Willats WGT. 2007. High-throughput microarray analysis of pectic polymers by enzymatic epitope deletion. Carbohydr. Polym. 70: 77−81. DOI: 10.1016/j.carbpol.2007.03.008.

Öhman D, Demedts B, Kumar M, Gerber L, Gorzsás A, Goeminne G, Hedenström M, Ellis B, Boerjan W, Sundberg B. 2013. MYB103 is required for ferulate-5-hydroxylase expression and syringyl lignin biosynthesis in *Arabidopsis* stems. Plant J. 73: 63−76. DOI:10.1111/tpj.12018.

Oldenbourg R. 2013. Polarized light microscopy: principles and practice. Cold Spring Harb. Protoc. 11: 1023−1036. DOI:10.1101/pdb.top078600.

Olins JR, Lin L, Lee SJ, Trabucco GM, MacKinnon KJM, Hazen SP. 2018. Secondary wall regulating NACs differentially bind at the promoter at a cellulose synthase A4 CiseQTL. Front. Plant Sci. 9: 1895. DOI:10.3389/fpls.2018.01895.

Ozparpucu M, Ruggeberg M, Gierlinger N, Cesarino I, Vanholme R, Boerjan W, Burgert I. 2017. Unravelling the impact of lignin on cell wall mechanics: a comprehensive study on young poplar trees downregulated for cinnamyl alcohol dehydrogenase (CAD). Plant J. 91: 480–490. DOI:10.1111/tpj.13584.

Pattathil S, Avci U, Baldwin D, Swennes AG, McGill JA, *et al*. 2010. A comprehensive toolkit of plant cell wall glycan-directed monoclonal antibodies. Plant Physiol. 153: 514–525. DOI:10.1104/pp.109.151985.

Patten AM, Cardenas CL, Cochrane FC, Laskar DD, Bedgar DL, Davin LB, Lewis NG. 2005. Reassessment of effects on lignification and vascular development in the irx4 *Arabidopsis* mutant. Phytochemistry 66: 2092–2107. DOI: 10.1016/j.phytochem.2004.12.016.

Pendle A, Benitez-Alfonso Y. 2015. Immunofluorescence detection of callose deposition around plasmodesmata sites. In: M Heinlein (ed.), Plasmodesmata: methods and protocols: 95–104. Springer, New York, USA.

Perera PN, Schmidt M, Chiang VL, Schuck PJ, Adams PD. 2012. Raman-spectroscopy-based noninvasive microanalysis of native lignin structure. Anal. Bioanal. Chem. 402: 983–987. DOI:10.1007/s00216-011-5518-x

Persson S, Sørensen I, Möller I, Willats W, Pauly M. 2010. Dissection of plant cell walls by high-throughput methods. In: P Ulvskov (ed.), Annual Plant Reviews: 43–64. Wiley-Blackwell, New Jersey, USA.

Pohling C, Brackmann C, Duarte A, Buckup T, Enejder A, Motzkus M. 2014. Chemical imaging of lignocellulosic biomass by CARS microscopy. J. Biophotonics. 7: 126–134. DOI:10.1002/jbio.201300052.

Potocka I, Godel K, Dobrowolska I, Kurczyńska EU. 2018. Spatio-temporal localization of selected pectic and arabinogalactan protein epitopes and the ultrastructural characteristics of explant cells that accompany the changes in the cell fate during somatic embryogenesis in *Arabidopsis thaliana*. Plant Physiol. Biochem. 127: 573–589. DOI: 10.1016/j.plaphy.2018.04.032.

Preston RD. 1974. The physical biology of plant cell walls. Chapman and Hall, London, United Kingdom.

Putoczki TL, Gerrard JA, Butterfield BG, Jackson SL. 2008. The distribution of un-esterified and methyl-esterified pectic polysaccharides in *Pinus radiata*. IAWA J. 29: 115–127. DOI:10.1163/22941932-90000173.

Qi G, Hu RB, Yu L, Chai GH, Cao YP, Zuo R, Kong YZ, Zhou GK. 2013. Two poplar cellulose synthase-like D genes, PdCSLD5 and PdCSLD6, are functionally conserved with *Arabidopsis* CSLD3. J. Plant Physiol. 170: 1267–1276. DOI: 10.1016/j.jplph.2013.04.014.

Qin L, Zhang YW, Liu YQ, He HX, Han MM, Li YY, Zeng MM, Wang XD. 2018. Recent advances in matrix-assisted laser desorption/ionisation mass spectrometry imaging (MALDI-MSI) for in situ analysis of endogenous molecules in plants. Phytochem. Anal. 29: 351–364. DOI:10.1002/pca.2759.

Qiu D, Wilson IW, Gan S, Washusen R, Moran GF, Southerton SG. 2008. Gene expression in *Eucalyptus* branch wood with marked variation in cellulose microfibril orientation and lacking G-layers. New Phytol. 179: 94–103. DOI:10.1111/j.1469-8137.2008.02439.x.

Reiterer A, Lichtenegger H, Tschegg S, Fratzl P. 1999. Experimental evidence for a mechanical function of the cellulose microfibril angle in wood cell walls. Philos. Mag. A. 79: 2173–2184. doiDOI:10.1080/01418619908210415

Reza M, Kontturi E, Jaaskelainen AS, Vuorinen T, Ruokolainen J. 2015. Transmission electron microscopy for wood and fiber analysis - a review. Bioresources. 10:6230–6261.

Reza M, Rojas LG, Kontturi E, Vuorinen T, Ruokolainen J. 2014. Accessibility of cell wall lignin in solvent extraction of ultrathin spruce wood sections. ACS Sustain. Chem. Eng. 2: 804–808. DOI:10.1021/sc400470m.

Richardson DS, Lichtman JW. 2015. Clarifying tissue clearing. Cell. 162: 246–257. DOI: 10.1016/j.cell.2015.06.067.

Richter S, Mussig J, Gierlinger N. 2011. Functional plant cell wall design revealed by the Raman imaging approach. Planta. 233: 763–772. DOI:10.1007/s00425-010-1338-z.

Ruel K, Nishiyama Y, Joseleau JP. 2012. Crystalline and amorphous cellulose in the secondary walls of *Arabidopsis*. Plant Sci. 193: 48–61. DOI: 10.1016/j.plantsci.2012.05.008.

Ruggeberg M, Saxe F, Metzger TH, Sundberg B, Fratzl P, Burgert I. 2013. Enhanced cellulose orientation analysis in complex model plant tissues. J. Struct. Biol. 183: 419–428. DOI: 10.1016/j.jsb.2013.07.001.

Running MP, Clark SE, Meyerowitz EM. 1995. Confocal microscopy of the shoot apex. Methods Cell Biol. 49: 217–229. DOI:10.1016/s0091-679x(08)61456-9.

Sandquist D, Norell L, Takabe K, Yoshinaga A, Daniel G. 2015. Anatomical and immune-coverage observations on SuSy, C4H, and pectate lyase family protein downregulated aspens genotypes. Bioresources. 10: 5016–5029.

Sarkanen KV, Hergert HL. 1971. Classification and distribution. In: KV Sarkanen, CH Ludwig (ed.), Lignins, occurrence, formation, structure and reactions: 43–49. Wiley Interscience, New York.

Sato S, Kato T, Kakegawa K, Ishii T, Liu YG, *et al*. 2001. Role of the putative membrane bound endo-1,4-β-glucanase KORRIGAN in cell elongation and cellulose synthesis in *Arabidopsis thaliana*. Plant Cell Physiol. 42: 251–263. DOI: 10.1093/pcp/pce045.

Saxe F, Eder M, Benecke G, Aichmayer B, Fratzl P, Burgert I, Ruggeberg M. 2014. Measuring the distribution of cellulose microfibril angles in primary cell walls by small angle X-ray scattering. Plant Methods. 10: 25. DOI:10.1186/1746-4811-10-25.

Schenk HJ, Espino S, Rich-Cavazos SM, Jansen S. 2018. From the sap's perspective: the nature of vessel surfaces in angiosperm xylem. Am. J. Bot. 105: 172–185. DOI:10.1002/ajb2.1034.

Schmidt M, Schwartzberg AM, Carroll A, Chaibang A, Adams PD, Schuck PJ. 2010. Raman imaging of cell wall polymers in *Arabidopsis thaliana*. Biochem. Biophys. Res. Commun. 395: 521–523. DOI: 10.1016/j.bbrc.2010.04.055.

Shchukarev A, Sundberg B, Mellerowicz E, Persson P. 2002. XPS study of living tree. Surf. Interface Anal. 34: 284–288. DOI:10.1002/sia.1301.

Siebers AM. 1960. The detection of tension wood with fluorescent dyes. Stain Technol. 35: 247–251. DOI:10.3109/10520296009114744.

Singh AP, Dawson BSW. 2014. FE-SEM characterisation of *Pinus radiata* solid wood and plywood surfaces following machining. IAWA J. 35: 69–84. DOI:10.1163/22941932-00000049.

Singhal N, Kumar M, Kanaujia PK, Virdi JS. 2015. MALDI-TOF mass spectrometry: an emerging technology for microbial identification and diagnosis. Front. Microbiol. 6: 791. DOI:10.3389/fmicb.2015.00791.

Sinn G, Reiterer A, Stanzl-Tschegg SE. 2001. Surface analysis of different wood species using X-ray photoelectron spectroscopy (XPS). J. Mater. Sci. 36: 4673–4680. DOI: 10.1023/a:1017954300015.

Smetana O, Makila R, Lyu M, Amiryousefi A, Rodriguez FS, *et al*. 2019. High levels of auxin signalling define the stem-cell organizer of the vascular cambium. Nature. 565: 485–489. DOI:10.1038/s41586-018-0837-0.

Snegireva AV, Ageeva MV, Amenitskii SI, Chernova TE, Ebskamp M, Gorshkova TA. 2010. Intrusive growth of sclerenchyma fibers. Russ. J. Plant Physiol. 57: 342–355. DOI:10.1134/s1021443710030052.

Sotiriou P, Giannoutsou E, Panteris E, Apostolakos P, Galatis B. 2016. Cell wall matrix polysaccharide distribution and cortical microtubule organization: two factors controlling mesophyll cell morphogenesis in land plants. Ann. Bot. 117: 401–419. DOI:10.1093/aob/mcv187.

Spokevicius A, Taylor L, Melder E, Van Beveren K, Tibbits J, Creux N, Bossinger G. 2016. The use of induced somatic sector analysis (ISSA) for studying genes and promoters involved in wood formation and secondary stem development. J Vis Exp. 116: e54553. DOI:10.3791/54553.

Spokevicius AV, Southerton SG, MacMillan CP, Qiu D, Gan S, Tibbits JFG, Moran GF, Bossinger G. 2007. β-tubulin affects cellulose microfibril orientation in plant secondary fibre cell walls. Plant J. 51: 717–726. DOI:10.1111/j.1365313X.2007.03176.x.

Stone BA, Evans NA, Bonig I, Clarke AE. 1984. The application of Sirofluor, a chemically defined fluorochrome from aniline blue for the histochemical detection of callose. Protoplasma 122: 191–195. DOI:10.1007/bf01281696.

Streit W, Fengel D. 1994. Heartwood formation in Quebracho colorado (*Schinopsis balansae* Engl.) - tannin distribution and penetration of extractives into the cell walls. Holzforschung 48: 361–367. DOI:10.1515/hfsg.1994.48.5.361.

Sturtevant D, Lee YJ, Chapman KD. 2016. Matrix assisted laser desorption/ionization-mass spectrometry imaging (MALDI-MSI) for direct visualization of plant metabolites in situ. Curr. Opin. Biotechnol. 37: 53–60. DOI: 10.1016/j.copbio.2015.10.004.

Sutherland P, Hallett I, Jones M. 2009. Probing cell wall structure and development by the use of antibodies: a personal perspective. NZ. J. For. Sci. 39: 197–205. DOI:10.1080/03014220909510579.

Svedström K, Lucenius J, Van den Bulcke J, Van Loo D, Immerzeel P, *et al*. 2012. Hierarchical structure of juvenile hybrid aspen xylem revealed using X-ray scattering and microtomography. Trees 26: 1793–1804. DOI:10.1007/s00468-012-0748-x.

Taguchi A, Murata K, Nakano T. 2010. Observation of cell shapes in wood cross-sections during water adsorption by confocal laser-scanning microscopy (CLSM). Holzforschung 64: 627–631. DOI:10.1515/hf.2010.092.

Takata N, Awano T, Nakata MT, Sano Y, Sakamoto S, Mitsuda N, Taniguchi T. 2019. *Populus* NST/SND orthologs are key regulators of secondary cell wall formation in wood fibers, phloem fibers and xylem ray parenchyma cells. Tree Physiol. 39: 514–525. DOI:10.1093/treephys/tpz004.

Thomas J, Idris NA, Collings DA. 2017. Pontamine fast scarlet 4B bifluorescence and measurements of cellulose microfibril angles. J. Microsc. 268: 13–27. DOI:10.1111/jmi.12582.

Thomas J, Ingerfeld M, Nair H, Chauhan SS, Collings DA. 2013. Pontamine fast scarlet 4B: a new fluorescent dye for visualising cell wall organisation in radiata pine tracheids. Wood Sci. Technol. 47: 59–75. DOI:10.1007/s00226-012-0483-x.

Thorn K. 2016. A quick guide to light microscopy in cell biology. Mol. Biol. Cell. 27: 219–222. DOI:10.1091/mbc.E15-02-0088.

Tuominen H, Puech L, Fink S, Sundberg B. 1997. A radial concentration gradient of indole-3-acetic acid is related to secondary xylem development in hybrid aspen. Plant Physiol. 115: 577–585. DOI:10.1104/pp.115.2.577.

Ursache R, Andersen TG, Marhavý P, Geldner N. 2018. A protocol for combining fluorescent proteins with histological stains for diverse cell wall components. Plant J. 93: 399–412. DOI:10.1111/tpj.13784.

Verbelen JP, Kerstens S. 2000. Polarization confocal microscopy and congo red fluorescence: a simple and rapid method to determine the mean cellulose fibril orientation in plants. J. Microsc. 198: 101–107. DOI:10.1046/j.1365-2818.2000.00691.x.

Verhertbruggen Y, Walker JL, Guillon F, Scheller HV. 2017. A comparative study of sample preparation for staining and immunodetection of plant cell walls by light microscopy. Front. Plant Sci. 8: 1505. DOI:10.3389/fpls.2017.01505.

Wang P, Calvo-Polanco M, Reyt G, Barberon M, Champeyroux C, *et al*. 2019. Surveillance of cell wall diffusion barrier integrity modulates water and solute transport in plants. Sci. Rep. 9: 4227. DOI:10.1038/s41598-019-40588-5.

Wang SC, Li EY, Porth I, Chen JG, Mansfield SD, Douglas CJ. 2015. Regulation of secondary cell wall biosynthesis by poplar R2R3 MYB transcription factor PtrMYB152 in *Arabidopsis*. Sci. Rep. 4: 5054. DOI:10.1038/srep05054.

Wessels B, Seyfferth C, Escamez S, Vain T, Antos K, *et al*. 2019. An AP2/ERF transcription factor ERF139 coordinates xylem cell expansion and secondary cell wall deposition. New Phytol. 224: 1585–1599. DOI:10.1111/nph.15960.

Willats WGT, Marcus SE, Knox JP. 1998. Generation of a monoclonal antibody specific to (1→5)-α-L-arabinan. Carbohydr. Res. 308: 149–152. DOI:10.1016/s00086215(98)00070-6.

Willats WGT, Steele-King CG, McCartney L, Orfila C, Marcus SE, Knox JP. 2000. Making and using antibody probes to study plant cell walls. Plant Physiol. Biochem. 38: 27–36. DOI:10.1016/s0981-9428(00)00170-4.

Wilson L, Tonkin M, Bossinger G. 2005. Transpiration-assisted perfusion fixation provides in situ preservation of developing ray parenchyma cells in *Eucalyptus nitens*. J. Microsc. 220: 113–119. DOI:10.1111/j.1365-2818.2005.01524.x.

Wood IP, Pearson BM, Garcia-Gutierrez E, Havlickova L, He Z, Harper AL, Bancroft I, Waldron KW. 2017. Carbohydrate microarrays and their use for the identification of molecular markers for plant cell wall composition. PNAS 114: 6860–6865. DOI:10.1073/pnas.1619033114.

Wood PJ. 1980. Specificity in the interaction of direct dyes with polysaccharides. Carbohydr. Res. 85: 271–287. DOI:10.1016/s0008-6215(00)84676-5.

Wu AM, Rihouey C, Seveno M, Hornblad E, Singh SK, Matsunaga T, Ishii T, Lerouge P, Marchant A. 2009. The *Arabidopsis* IRX10 and IRX10-LIKE glycosyltransferases are critical for glucuronoxylan biosynthesis during secondary cell wall formation. Plant J. 57: 718–731. DOI:10.1111/j.1365-313X.2008.03724.x.

Xu P, Donaldson L, Walker J, Evans R, Downes G. 2004. Effects of density and microfibril orientation on the vertical variation of low-stiffness wood in radiata pine butt logs. Holzforschung. 58: 673–677. DOI: 10.1515/hf.2004.122.

Xu P, Donaldson LA, Gergely ZR, Staehelin LA. 2006. Dual-axis electron tomography: a new approach for investigating the spatial organization of wood cellulose microfibrils. Wood Sci Technol. 41: 101–116. DOI: 10.1007/s00226-006-0088-3.

Xu P, Liu H, Donaldson LA, Zhang Y. 2011. Mechanical performance and cellulose microfibrils in wood with high S2 microfibril angles. J. Mater. Sci. 46: 534–540. DOI: 10.1007/s10853-010-5000-8.

Xu P, Liu H, Evans R, Donaldson LA. 2009. Longitudinal shrinkage behaviour of compression wood in radiata pine. Wood Sci Technol. 43: 423–439. DOI: 10.1007/s00226-008-0228-z.

Yang F, Mitra P, Zhang L, Prak L, Verhertbruggen Y, *et al*. 2013. Engineering secondary cell wall deposition in plants. Plant Biotechnol. J. 11: 325–335. DOI:10.1111/pbi.12016.

Yang L, Zhao X, Ran LY, Li CF, Fan D, Luo KM. 2017. PtoMYB156 is involved in negative regulation of phenylpropanoid metabolism and secondary cell wall biosynthesis during wood formation in poplar. Sci. Rep. 7: 41209. DOI:10.1038/srep41209.

Ye ZH, Zhong RQ. 2015. Molecular control of wood formation in trees. J. Exp. Bot. 66: 4119–4131. DOI:10.1093/jxb/erv081.

Yeung ECT, Stasolla C, Sumner MJ, Huang BQ. 2015. Plant microtechniques and protocols. Springer, Switzerland.

Yoshinaga A, Kamitakahara H, Takabe K. 2016. Distribution of coniferin in differentiating normal and compression woods using MALDI mass spectrometric imaging coupled with osmium tetroxide vapor treatment. Tree Physiol. 36: 643–652. DOI:10.1093/treephys/tpv116.

Yuan HM, Zhao LJ, Guo WD, Yu Y, Tao L, *et al*. 2019. Exogenous application of phytohormones promotes growth and regulates expression of wood formation-related genes in *Populus simonii* x *P. nigra*. Int. J. Mol. Sci. 20: 792. DOI:10.3390/ijms20030792.

Zhang J, Xie M, Tuskan GA, Muchero W, Chen J. 2018. Recent advances in the transcriptional regulation of secondary cell wall biosynthesis in the woody plants. Front. Plant Sci. 9: 1535. DOI:10.3389/fpls.2018.01535.

Zhang X, Chen S, Xu F. 2017. Combining Raman imaging and multivariate analysis to visualize lignin, cellulose, and hemicellulose in the plant cell wall. J. Vis. Exp. 124: e55910. DOI:10.3791/55910.

Zhang Y, Brown G, Whetten R, Loopstra CA, Neale D, Kieliszewski MJ, Sederoff RR. 2003. An arabinogalactan protein associated with secondary cell wall formation in differentiating xylem of loblolly pine. Plant Mol. Biol. 52: 91–102. DOI: 10.1023/a:1023978210001.

Zhong RQ, Cui DT, Ye ZH. 2019. Secondary cell wall biosynthesis. New Phytol. 221: 1703–1723. DOI:10.1111/nph.15537.

Zhong RQ, Lee CH, Ye ZH. 2010. Evolutionary conservation of the transcriptional network regulating secondary cell wall biosynthesis. rends Plant Sci. 15: 625–632. DOI:10.1016/j.tplants.2010.08.007.

Zhong RQ, Ye ZH. 2013. Transcriptional regulation of wood formation in tree species. In: J Fromm (ed.), Cellular aspects of wood formation: 141–158. Springer-Verlag Berlin Heidelberg Germany.

Zhong RQ, Ye ZH. 2014. Complexity of the transcriptional network controlling secondary wall biosynthesis. Plant Sci. 229: 193–207. DOI: 10.1016/j.plantsci.2014.09.009.

Zhong RQ, Ye ZH. 2015. Secondary cell walls: biosynthesis, patterned deposition and transcriptional regulation. Plant Cell Physiol. 56: 195–214. DOI:10.1093/pcp/pcu140.

Zuo Y, Gu J, Tan H, Zhang D, Li P, Zhang Y. 2012. The application of X-ray photoelectron spectroscopy technology in wood adhesives. In: W Zhang (ed.), Software engineering and knowledge engineering: theory and practice: 829–835. Springer-Verlag, Berlin, Heidelberg, Germany.